

# Critical Exponents of the 3D Ising Universality Class From Finite Size Scaling With Standard and Improved Actions

M. Hasenbusch<sup>a</sup>, K. Pinn<sup>b</sup>, and S. Vinti<sup>b</sup>

<sup>a</sup> Fachbereich Physik, Humboldt-Universität zu Berlin  
Invalidenstr. 110, D-10099 Berlin, Germany  
e-mail: [hasenbus@ficus1.physik.hu-berlin.de](mailto:hasenbus@ficus1.physik.hu-berlin.de)

<sup>b</sup> Institut für Theoretische Physik I, Universität Münster  
Wilhelm-Klemm-Str. 9, D-48149 Münster, Germany  
e-mail: [pinn@uni-muenster.de](mailto:pinn@uni-muenster.de), [vinti@uni-muenster.de](mailto:vinti@uni-muenster.de)

## Abstract

We propose a method to obtain an improved Hamiltonian (action) for the Ising universality class in three dimensions. The improved Hamiltonian has suppressed leading corrections to scaling. It is obtained by tuning models with two coupling constants. We studied three different models: the  $\pm 1$  Ising model with nearest neighbour and body diagonal interaction, the spin-1 model with states  $0, \pm 1$ , and nearest neighbour interaction, and  $\phi^4$ -theory on the lattice (Landau-Ginzburg Hamiltonian). The remarkable finite size scaling properties of the suitably tuned spin-1 model are compared in detail with those of the standard Ising model. Great care is taken to estimate the systematic errors from residual corrections to scaling. Our best estimates for the critical exponents are  $\nu = 0.6298(5)$  and  $\eta = 0.0366(8)$ , where the given error estimates take into account the statistical and systematic uncertainties.

# Contents

|          |   |           |
|----------|---|-----------|
| <b>1</b> | <b>Introduction</b>   | <b>4</b>  |
| <b>2</b> | <b>Improving the Scaling Behaviour</b>                      | <b>5</b>  |
| 2.1      | The Models . . . . .  | 5         |
| 2.2      | Matching of Phenomenological Couplings . . . . .            | 6         |
| 2.3      | RG Analysis of the Matching Condition . . . . .             | 7         |
| 2.4      | Computing the Matching Flows . . . . .                      | 9         |
| 2.5      | Identification of the $u_2 = 0$ Line . . . . .              | 11        |
| <b>3</b> | <b>Simulation Parameters and Statistics</b>                 | <b>12</b> |
| 3.1      | Standard Action . . . . .                                   | 12        |
| 3.2      | Improved Action . . . . .                                   | 14        |
| <b>4</b> | <b>Measured Quantities and Basic Data</b>                   | <b>16</b> |
| <b>5</b> | <b>Fitting the Data</b>                                     | <b>17</b> |
| 5.1      | $R_2$ at fixed $R_1$ . . . . .                              | 22        |
| 5.2      | Fitting $R_1$ and $R_2$ . . . . .                           | 24        |
| 5.2.1    | Standard Action, Fit $R_i$ . . . . .                        | 24        |
| 5.2.2    | Improved Action, Fit $R_i$ . . . . .                        | 29        |
| 5.3      | Fitting the Derivatives of the $R_i$ . . . . .              | 34        |
| 5.3.1    | Standard Action, Fit $dR_i/d\beta$ . . . . .                | 34        |
| 5.3.2    | Improved Action, Fit $\partial R_i/\partial\beta$ . . . . . | 37        |
| 5.4      | Fitting the Susceptibility . . . . .                        | 41        |
| 5.4.1    | Standard Action, Fit $\chi$ . . . . .                       | 41        |
| 5.4.2    | Improved Action, Fit $\chi$ . . . . .                       | 43        |
| 5.5      | Fitting the Energy . . . . .                                | 45        |
| 5.5.1    | Improved Action, Fit $E$ . . . . .                          | 45        |
| 5.5.2    | Standard Action, Fit $E$ . . . . .                          | 45        |
| <b>6</b> | <b>Comparison with Other Estimates</b>                      | <b>47</b> |
| <b>7</b> | <b>Conclusions</b>  | <b>49</b> |

## List of Tables

|    |  |    |
|----|--|----|
| 1  | Flows of couplings from matching condition . . . . .                                   | 10 |
| 2  | Testing the wall cluster algorithm . . . . .   | 13 |
| 3  | Simulation parameters and statistics . . . . .   | 15 |
| 4  | IA, fit $\bar{Q}$ with correction to scaling term . . . . .                            | 23 |
| 5  | SA, fit $\bar{Q}$ with correction to scaling terms . . . . .                           | 23 |
| 6  | SA, fit $R_i$ separately, with $\omega$ fixed . . . . .                                | 24 |
| 7  | SA, fit $R_2$ , with $\omega$ free . . . . .   | 25 |
| 8  | SA, fit $R_i$ simultaneously, with $\omega$ free and extra $x$ for $R_2$ . . . . .     | 28 |
| 9  | IA, fit $R_i$ separately, no correction to scaling . . . . .                           | 30 |
| 10 | IA, fit $R_i$ simultaneously, no correction to scaling . . . . .                       | 30 |
| 11 | IA, fit $R_i$ simultaneously, with correction to scaling . . . . .                     | 31 |
| 12 | SA, fit $dR_i/d\beta$ , no correction to scaling . . . . .                             | 34 |
| 13 | SA, fit $dR_2/d\beta$ , with $\omega$ fixed . . . . .                                  | 35 |
| 14 | SA, fit $dR_1/d\beta$ with leading and higher correction . . . . .                     | 36 |
| 15 | IA, fit $\partial R_i/\partial\beta$ , no correction to scaling . . . . .              | 38 |
| 16 | IA, fit $\partial R_i/\partial\beta$ , with correction to scaling . . . . .            | 39 |
| 17 | SA, fit $\chi$ at fixed $Q$ . . . . .  | 42 |
| 18 | SA, fit $\chi$ at fixed $Z_a/Z_p$ . . . . .  | 42 |
| 19 | IA, fit $\chi$ at fixed $Q$ . . . . .  | 43 |
| 20 | IA, fit $\chi$ at fixed $Z_a/Z_p$ . . . . .  | 43 |
| 21 | IA, fit energy, no correction to scaling . . . . .                                     | 46 |
| 22 | SA, fit energy, no correction to scaling . . . . .                                     | 46 |
| 23 | SA, fit energy, with correction to scaling . . . . .                                   | 46 |
| 24 | Comparing Exponent Estimates with Previous Ones . . . . .                              | 48 |
| 25 | SA, Monte Carlo estimates for $R_1$ , $R_2$ , $\chi$ , and $E_{NN}$ . . . . .          | 52 |
| 26 | IA, Monte Carlo estimates for $R_1$ , $R_2$ and $\chi$ . . . . .                       | 53 |
| 27 | IA, Monte Carlo estimates for energies $E_{NN}$ , $E_D$ and $E$ . . . . .              | 54 |
| 28 | SA, Monte Carlo estimates for $dR_i/d\beta$ . . . . .                                  | 55 |
| 29 | IA, Monte Carlo estimates for $\partial R_i/\partial\beta$ and $dR_i/d\beta$ . . . . . | 56 |

IA: Improved Action

SA: Standard Action

## List of Figures

|    |  |    |
|----|--|----|
| 1  | IA & SA, plot of $R_2 = Q$ . . . . .   | 18 |
| 2  | IA & SA, plot of $R_1 = Z_a/Z_p$ . . . . .   | 19 |
| 3  | IA & SA, plot of $\beta$ derivatives of $Q$ and plot of $\chi$ . . . . .                 | 20 |
| 4  | SA, $R_1^*$ and $\beta_c$ from fit with fixed $\omega$ . . . . .                         | 26 |
| 5  | SA, $R_2^*$ and $\beta_c$ , with $\omega$ fixed and $\omega$ free . . . . .              | 27 |
| 6  | IA, $R_2^*$ and $\beta_c$ from simultaneous fit of $R_i$ . . . . .                       | 32 |
| 7  | SA, $\nu$ from $dR_2/d\beta$ , without and with correction to scaling . .                | 36 |
| 8  | IA, $\nu$ from $\partial R_i/\partial\beta$ . . . . .                                    | 38 |
| 9  | IA, $\nu$ from $\partial R_1/\partial\beta$ , without and with correction to scaling . . | 39 |
| 10 | IA, $\nu$ from $\partial R_2/\partial\beta$ , $\beta$ -dependence . . . . .              | 40 |
| 11 | IA, $\eta$ from $\chi$ at fixed $Z_a/Z_p$ . . . . .                                      | 44 |
| 12 | IA & SA, $\nu$ from energy . . . . .   | 47 |

IA: Improved Action

SA: Standard Action

# 1 Introduction

In Monte Carlo simulations the size of the systems that can be studied is limited by the memory of the computer and by the CPU-time that is available. Therefore, in many instances, finite size scaling [1] is the key to a precise determination of properties of statistical systems at criticality. Finite size scaling laws are affected by corrections to scaling. These corrections to scaling cause systematic errors in the results for the infinite volume limit one is interested in. With improving statistical accuracy of the Monte Carlo data it becomes important to deal properly with systematic errors. One way to proceed is to include corrections to scaling into the fit ansätze when analysing the data. Another, more fundamental way is to remove corrections already from the system to be studied.

Renormalization group (RG) [2] offers (at least in principle) a way to achieve this goal. RG fixed point actions\* are free of corrections to scaling. However such actions in general contain an infinite number of couplings. In practical applications one is forced to truncate the action to a finite number of terms, which in fact is an uncontrolled approximation. For an application of this strategy to asymptotically free models see the work on Perfect Actions [3].

A different approach was pioneered by K. Symanzik [4]. Higher order terms are added to the action. By imposing certain conditions on observables leading corrections to scaling are eliminated. While Symanzik formulated his method in the framework of perturbation theory, recently there have been attempts to apply this method in a non-perturbative, i.e. numerical, setting [5].

Our present approach is closer to this latter point of view than to the block spin renormalization group inspired framework.

The idea to improve the scaling properties of Ising models by moving to models with generalized actions and tuning the coupling constants as to obtain reduced corrections to scaling was already followed in the work of Blöte et al. [6]. However, in their work they do not uncover the principle and method they used to obtain their improved actions.

In a recent paper [7], we presented data obtained with a spin-1 Ising model with states  $0, \pm 1$ . Tuning the two coupling constants in the proper

---

\*What is called Hamiltonian or energy function in Statistical Mechanics is called Action in Euclidean Field Theory.

way, we were able to reduce the corrections to scaling in various quantities dramatically. Especially the Binder cumulant and its derivatives, and also the susceptibility, could be fitted with scaling laws without corrections to scaling terms, yielding very precise estimates of the 3D Ising critical exponents.

Recently the authors of refs. [8, 9] argued that the improvement discussed above does not lead to reduced error estimates for critical exponents. They argue that the error estimates given in our recent paper [7] are underestimated, since we do not take into account residual leading correction to scaling corrections. Such corrections might well be present, since the parameters of our improved model are computed numerically. However, this is not the full story as we shall explain in this paper. Our argument is based on the fact that ratios of correction to scaling amplitudes are universal.

In this article, we describe in detail our method, the numerical results, and the fitting procedures. We confront the results from the improved actions with high precision data from simulations of the standard Ising model, estimating with a well defined procedure systematic errors for both actions.

## 2 Improving the Scaling Behaviour

### 2.1 The Models

Usually, Monte Carlo studies of the Ising model are done using what in field theory is called

#### Standard Action

$$S = -\beta \sum_{\langle i,j \rangle} s_i s_j. \quad (1)$$

The  $s_i$  take values  $\pm 1$ , and the spin-spin interaction is a sum over all nearest neighbour pairs  $\langle i, j \rangle$ . A precise estimate for the critical coupling was obtained in reference [10]:  $\beta_c = 0.2216544(3)(3)$ .

In the following we will introduce and study three different models in the 3D Ising universality class, each of them governed by *two* coupling constants. In all three cases the Boltzmann factor is given by  $\exp(-S)$ .

#### Spin-1 Model

$$S = -\beta \sum_{\langle i,j \rangle} s_i s_j + D \sum_i s_i^2. \quad (2)$$

The  $s_i$  take values  $0, \pm 1$ , and the spin-spin interaction is a sum over all nearest neighbour pairs. This model was introduced and studied in [6]. There,  $D$  was fixed to  $\ln 2$ . The critical  $\beta$  corresponding to this particular value of  $D$  was estimated in [6] to be  $\beta_c = 0.3934224(10)$ .

### NNN Model

$$S = -\beta_1 \sum_{\langle i,j \rangle} s_i s_j - \beta_2 \sum_{[i,j]} s_i s_j. \quad (3)$$

The  $s_i$  take values  $\pm 1$ , and the spin-spin interaction is a sum over all nearest neighbour pairs  $\langle i, j \rangle$  and third neighbour pairs (body diagonals)  $[i, j]$ . Blöte et al. fixed  $\beta_2/\beta_1 = 0.4$  and obtained  $\beta_{1,c} = 0.1280036(5)$ .

### $\phi^4$ -Model

$$S = -\beta \sum_{\langle i,j \rangle} \phi_i \phi_j + \sum_i \phi_i^2 + \lambda \sum_i (\phi_i^2 - 1)^2. \quad (4)$$

The variables  $\phi$  assume real values. In the limit  $\lambda \rightarrow \infty$  one recovers the standard Ising model.

The three models defined above have in common that they have a second order critical line in the space spanned by the two coupling constants. We exploit the degree of freedom of moving on the critical line to find critical models with reduced corrections to scaling. How this is done will be explained in the following subsections.

## 2.2 Matching of Phenomenological Couplings

We study two independent phenomenological couplings of the 3D Ising model, to be called  $R_i$ ,  $i = 1, 2$  in the following. Both quantities are universal, i.e. at criticality their infinite volume limit  $R_i^*$  does not depend on details of the microscopic Hamiltonian.  $R_1$  is the ratio of partition functions with anti-periodic and periodic boundary conditions, respectively,

$$R_1 = Z_a/Z_p. \quad (5)$$

The lattices will always be cubical with extension  $L$  in each of the three directions. Antiperiodic boundary conditions are imposed only in one of the three lattice directions.  $R_2$  is the Binder cumulant,

$$R_2 = Q = \frac{\langle m^2 \rangle^2}{\langle m^4 \rangle}. \quad (6)$$

Here,  $m$  denotes the magnetization per spin,

$$m = L^{-3} \sum_i s_i. \quad (7)$$

The  $R_i$  are  $L$ -dependent and, of course, functions of the coupling parameters in the action. For the two-coupling models defined above, we define “flows” (lines of constant physics)  $(K_1(L), K_2(L))$  by requiring that

$$R_i(L, K_1(L), K_2(L)) = R_i^*. \quad (8)$$

$K_1$  and  $K_2$  represent the two coupling constants of the model. In the next subsection we shall demonstrate that with increasing  $L$  the flows of  $(K_1, K_2)$  converge towards a critical point which has no leading order corrections to scaling.

### 2.3 RG Analysis of the Matching Condition

The main features of the two-coupling models can be discussed in the framework of the renormalization group. The scaling properties can be derived from the linearized RG transformation at the fixed point.

We consider general Hamiltonians with couplings  $K_\alpha$ , where  $\alpha = 1, 2, \dots$ . An RG transformation, realized, e.g., by a block spin transformation, changes these couplings according to

$$K \rightarrow K' = R(K) \equiv K'(K). \quad (9)$$

A fixed point  $K^*$  is defined through  $R(K^*) = K^*$ . The linearized transformation at the fixed point can be represented by a matrix

$$T_{\alpha\beta} = \left. \frac{\partial K'_\alpha}{\partial K_\beta} \right|_{K=K^*}. \quad (10)$$

One introduces “normal coordinates” (scaling fields) by

$$u_i = u_i(K) = \sum_\alpha \varphi_{i,\alpha} (K_\alpha - K_\alpha^*), \quad (11)$$

where  $\varphi_i$  denotes the  $i$ -th (left) eigenvector of the matrix  $T$ ,

$$\sum_\alpha \varphi_{i,\alpha} T_{\alpha\beta} = \lambda_i \varphi_{i,\beta}.$$

The  $u_i$  transform under RG transformations like

$$u_i \rightarrow \lambda_i u_i .$$

In Ising type models the leading eigenvalues are given by

$$\lambda_1 = b^{1/\nu} , \quad \lambda_2 = b^{-\omega} , \quad \lambda_3 = b^{-x} , \quad (12)$$

where  $x \gg \omega$ . Note that  $x = 2$  for the lattice Gaussian model. From leading order  $\epsilon$ -expansion one expects that  $x$  is close to 2 at the Wilson-Fisher fixed point.  $b$  denotes the scale factor of the RG transformation.

Let us now assume that we have only two non-vanishing couplings  $K_1$  and  $K_2$  in our Hamiltonian. Let us then write down explicitly the condition for being critical ( $u_1 = 0$ ) and eliminating the leading corrections to scaling ( $u_2 = 0$ ). The first condition reads

$$\varphi_{1,1}(K_1 - K_1^*) + \varphi_{1,2}(K_2 - K_2^*) = \kappa_{1,3} , \quad (13)$$

whereas the condition  $u_2 = 0$  translates to

$$\varphi_{2,1}(K_1 - K_1^*) + \varphi_{2,2}(K_2 - K_2^*) = \kappa_{2,3} . \quad (14)$$

For  $i = 1, 2$ , the  $\kappa_{i,3}$  are given by

$$\kappa_{i,3} = \sum_{\alpha \geq 3} \varphi_{i,\alpha} K_\alpha^* . \quad (15)$$

Let us now study how our matching procedure with the two quantities  $R_1 = Z_a/Z_p$  and  $R_2 = Q$  works. The  $R_k$  are functions of the bare couplings and the lattice size:

$$R_k = R_k(L, K_1, K_2) . \quad (16)$$

We express these quantities as functions of the scaling fields defined above,

$$R_k(L, K_1, K_2) = R_k \left( L^{1/\nu} u_1^{(1)} , L^{-\omega} u_2^{(1)} \right) . \quad (17)$$

Here, the upper index <sup>(1)</sup> indicates that the scaling field is taken at the scale of the lattice spacing. The prefactor promotes the scaling field to its value at the scale  $L$ . Taylor-expansion of the  $R_k$  around their fixed point values yields

$$R_k \approx R_k^* + r_{k,1} L^{1/\nu} u_1^{(1)} + r_{k,2} L^{-\omega} u_2^{(1)} . \quad (18)$$

The matching conditions  $R_k = R_k^*$  are thus equivalent to

$$r_{k,1}L^{1/\nu}u_1^{(1)} + r_{k,2}L^{-\omega}u_2^{(1)} = 0, \quad (19)$$

for  $k = 1, 2$ . We obtain, as desired, the solution  $u_1^{(1)} = 0$  (criticality) and  $u_2^{(1)} = 0$  (no leading order corrections). Including higher order corrections in the scaling ansatz, governed by  $u_3$  and exponent  $\lambda_3$ , one can convince oneself that fixing  $R_1$  and  $R_2$  to their fixed point values leads to convergence to the critical line  $u_1 = 0$  with corrections that decay like  $L^{-x-1/\nu}$ . The  $u_2 = 0$  condition is approached with a much slower rate, namely like  $L^{-x+\omega}$ .

## 2.4 Computing the Matching Flows

For the three 2-coupling models specified above, we set up a procedure to determine the flows of couplings  $(K_1(L), K_2(L))$  such that eq. (8) was fulfilled. To this end we used estimates for  $R_1^* = 0.5425(10)$  and  $R_2^* = 0.6240(10)$ , which were an outcome of a preliminary analysis of data obtained using the standard action.

The matching couplings were searched for using a Newton iteration, based on the inversion of a matrix made up from Monte Carlo estimates of the derivatives of the  $R_i$  with respect to the two couplings. Typically three to four iterations were sufficient to find couplings such that  $Z_a/Z_p$  and  $Q$  attained the prescribed values within the given statistical precision. The results are given in table 1.

A first look at the table reveals that both for the spin-1 and the  $\phi^4$ -model, the flow converges to a fixed point quickly, whereas it keeps moving strongly in the case of the NNN model. A rough explanation of this could be the following: In order to remove the leading corrections to scaling, one has to move efficiently between the Gaussian model (equivalent to the  $\phi^4$ -model with vanishing  $\lambda$ ) and the non-trivial Wilson-Fisher fixed point. Moving between these two fixed points is most efficiently done using a  $\phi^4$ -type coupling, which is implicitly present also in the spin-1 model. The NNN model seems to need renormalization to a larger scale in order to come close to the flow line connecting the Gaussian with the Wilson-Fisher fixed point.

Plotting the second coupling vs. the first one, one finds that with very good precision the critical line can be approximated by a straight line:

$$K_2(L) = a_1 + a_2 K_1(L), \quad (20)$$

with

| <b>Spin-1 Model</b>              |           |           |             |             |
|----------------------------------|-----------|-----------|-------------|-------------|
| $L$                              | $\beta$   | $D$       | $Z_a/Z_p$   | $Q$         |
| 3                                | 0.35737   | 0.4401    | 0.54201(30) | 0.62447(21) |
| 4                                | 0.37250   | 0.5510    | 0.54242(25) | 0.62347(18) |
| 5                                | 0.37794   | 0.5883    | 0.54292(19) | 0.62421(15) |
| 6                                | 0.38210   | 0.6169    | 0.54221(49) | 0.62426(35) |
| 7                                | 0.38419   | 0.6311    | 0.54326(30) | 0.62366(22) |
| 8                                | 0.38320   | 0.6241    | 0.54291(37) | 0.62430(27) |
| 9                                | 0.38320   | 0.6241    | 0.54259(60) | 0.62403(44) |
| 10                               | 0.38320   | 0.6241    | 0.54288(57) | 0.62431(42) |
| <b>NNN Model</b>                 |           |           |             |             |
| $L$                              | $\beta_1$ | $\beta_2$ | $Z_a/Z_p$   | $Q$         |
| 4                                | 0.12266   | 0.05406   | 0.5429(2)   | 0.6238(2)   |
| 5                                | 0.12928   | 0.05028   | 0.5427(1)   | 0.6241(2)   |
| 6                                | 0.13431   | 0.04734   | 0.5425(1)   | 0.62441(8)  |
| 7                                | 0.13800   | 0.04518   | 0.5425(3)   | 0.6242(2)   |
| 8                                | 0.14069   | 0.04361   | 0.5426(2)   | 0.6243(1)   |
| 9                                | 0.14292   | 0.04231   | 0.5430(2)   | 0.6232(1)   |
| 10                               | 0.14406   | 0.04165   | 0.5425(2)   | 0.6242(2)   |
| 11                               | 0.14590   | 0.04059   | 0.5429(1)   | 0.62385(8)  |
| 12                               | 0.14724   | 0.03981   | 0.5426(1)   | 0.6235(1)   |
| 13                               | 0.14808   | 0.03933   | 0.5431(1)   | 0.6236(1)   |
| <b><math>\phi^4</math>-Model</b> |           |           |             |             |
| $L$                              | $\beta$   | $\lambda$ | $Z_a/Z_p$   | $Q$         |
| 3                                | 0.35303   | 1.5248    | 0.5420(3)   | 0.6244(2)   |
| 4                                | 0.36338   | 1.3282    | 0.5425(3)   | 0.6243(2)   |
| 5                                | 0.36908   | 1.2188    | 0.5425(2)   | 0.6241(1)   |
| 6                                | 0.37165   | 1.1689    | 0.5427(2)   | 0.6241(1)   |
| 7                                | 0.37270   | 1.1481    | 0.5424(2)   | 0.6243(1)   |
| 8                                | 0.37308   | 1.1410    | 0.5421(1)   | 0.6245(1)   |
| 9                                | 0.37273   | 1.1479    | 0.5416(3)   | 0.6247(2)   |

Table 1: Flows of couplings defined such that for all lattice sizes the two quantities  $R_1 = Z_a/Z_p$  and  $R_2 = Q$  match (to the given statistical precision) with their fixed point values  $R_1^* = 0.5425(10)$  and  $R_2^* = 0.6240(10)$ .

| model    | $a_1$  | $a_2$   |
|----------|--------|---------|
| spin-1   | -2.04  | 6.95    |
| NNN      | 0.1253 | -0.5804 |
| $\phi^4$ | 8.29   | -19.17  |

It is assuring that for the spin-1 and the NNN model, the critical coupling estimates determined by Blöte et al. are in good agreement with our critical lines.

Fits of  $K_1(L)$  with a power law

$$K_1(L) = c_1 + c_2 L^{-\alpha} \quad (21)$$

yielded good fits in all cases, with exponents of order 3 in the cases of spin-1 and  $\phi^4$ -models. Note that this exponent is much larger than  $-x + \omega$  that is to be expected from the theory presented above. For the NNN model, the exponent is of order 1.

The slow convergence of the NNN flow motivated our decision to discard this model from further investigation. Also, the behaviour of the  $\phi^4$  and spin-1 models appears to be very similar. We decided to concentrate on the spin-1 model, and leave the  $\phi^4$ -model for later study.

Note that our result for the optimal  $\lambda \approx 1.145$  of the  $\phi^4$ -model is consistent with the observation of ref. [9] that the optimal  $\lambda$  should be close to one.

## 2.5 Identification of the $u_2 = 0$ Line

After the decision to concentrate on the spin-1 model, we determined an approximation of the  $u_2 = 0$  manifold. This was done by looking at the derivatives of the  $R_i$  at criticality. From the RG analysis of section 2.3 one infers

$$\frac{\partial R_k}{\partial K_\alpha} = \sum_i \frac{\partial R_k}{\partial u_i} \frac{\partial u_i}{\partial K_\alpha} = r_{k,1} L^{1/\nu} \varphi_{1,\alpha} + r_{k,2} L^{-\omega} \varphi_{2,\alpha}. \quad (22)$$

The left hand side of the equation can be determined by Monte Carlo simulation and will therefore be assumed as known. Taking into account that without loss of generality one can set  $\varphi_{i,1} \equiv 1$ , the equations can be solved (or fitted) if the left hand side is known at least for two different lattice sizes. We performed Monte Carlo simulations at  $(\beta, D) = (0.3832, 0.6241)$  for lattice size 8, 9, 10, and 11. Fixing the exponents  $\nu = 0.63$  and  $\omega = 0.81$  [11] we

obtained that the scaling field  $\phi_{2,2}$  should be approximately  $-1/3$ . Plugging this into the eq. (14),

$$\varphi_{2,1}(K_1 - K_1^*) + \varphi_{2,2}(K_2 - K_2^*) = \kappa_{2,3}, \quad (23)$$

one obtains that  $3\beta - D$  should be kept constant. We used our simulation point (0.3832,0.6241) to fix this constant. In conclusion, one should approach criticality by varying  $\beta$  while adjusting  $D$  according to

$$D = 3(\beta - 0.3832) + 0.6241. \quad (24)$$

Of course, a precise estimate of  $\beta_c$  along this line still has to be determined. This will be discussed in the next section.

The fit result for  $\varphi_{1,2}$  can be used to perform a consistency check. In terms of the scaling fields, the critical line is characterized by

$$(\beta - \beta^*) + \varphi_{1,2}(D - D^*) = 0, \quad (25)$$

ignoring all higher couplings. Solving for  $D$  and plugging in the “experimental values”  $\beta^* = 0.3832$ ,  $D^* = 0.6241$  and  $\varphi_{1,2} = -0.1439$  one obtains with good precision the critical line approximation  $D = -2.04 + 6.95\beta$ . Let us close this section by remarking that errors in the precise estimation of the  $u_2 = 0$  line affect results for the critical exponents only weakly, e.g., the effect on the exponent  $\nu$  is of order  $L^{-1/\nu-\omega}$ .

## 3 Simulation Parameters and Statistics

### 3.1 Standard Action

Monte Carlo simulations of the 3D Ising model with standard action were performed at  $\beta = 0.2216545$ , which is a good approximation of the critical coupling [6, 10].

For cubical lattices of size  $L = 2$  up to  $L = 19$  we performed simulations with the multi-spin demon update [12, 13]. The update algorithm is local. Hence one expects a dynamical critical exponent  $z \approx 2$ . However, due to the multi-spin coding implementation a single sweep can be done substantially faster than with the cluster algorithm. Therefore one expects a better performance for the demon update on such small lattices.

| $L$ | $M$    | $S/V$       | $\tau_E$ | $\tau_\chi$ | $\tau_b$ |
|-----|--------|-------------|----------|-------------|----------|
| 6   | 300000 | 0.38412(29) | 1.12(2)  | 1.18(2)     | 0.53(1)  |
| 8   | 300000 | 0.33222(27) | 1.13(2)  | 1.19(2)     | 0.56(1)  |
| 12  | 300000 | 0.27005(24) | 1.13(2)  | 1.18(2)     | 0.57(1)  |
| 16  | 300000 | 0.23277(23) | 1.17(2)  | 1.19(2)     | 0.58(1)  |
| 24  | 300000 | 0.18866(20) | 1.15(2)  | 1.13(2)     | 0.55(1)  |
| 32  | 700000 | 0.16214(13) | 1.18(2)  | 1.14(2)     | 0.56(1)  |
| 48  | 450000 | 0.13098(14) | 1.20(2)  | 1.09(2)     | 0.54(1)  |
| 64  | 600000 | 0.11258(11) | 1.26(2)  | 1.10(2)     | 0.55(1)  |
| 96  | 340000 | 0.09075(13) | 1.26(4)  | 1.05(3)     | 0.53(1)  |

Table 2: Testing the performance of the wall cluster algorithm.  $M$  denotes the number of measurements, separated by a single wall cluster step. The  $\tau$ 's are integrated autocorrelation times. The unit of time is set to one complete update of the lattice; i.e. one measurement/ $(S/V)$ .  $S/V$  denotes the average sum of the sizes of the flipped clusters, normalized to the lattice volume  $L^3$ .

For a subset of the smaller lattices, and for bigger lattices up to size 128, cluster update was performed, using a new variant of the algorithm, the *wall cluster algorithm*. Note that there is quite a lot of freedom in the selection of clusters which are flipped during one update step. In the wall cluster algorithm, one flips all clusters that intersect with a given lattice plane. Sequentially one takes lattice planes in  $1-2$ ,  $1-3$  and  $2-3$  direction. The position is chosen randomly. Let us call the procedure to generate and flip all the clusters connected to the selected plane a wall cluster update step. The motivation for choosing this type of update was that the construction of all clusters that have elements in a lattice plane is needed for the measurement of  $Z_a/Z_p$  anyway. Testing the performance of the algorithm shows that there is some small gain in efficiency compared to the single cluster update [14]. Results for cluster size distribution and relaxation times of simulations at  $\beta_c$  are given in table 2.

The average sum of the sizes of the clusters per volume that are flipped in one step behaves as

$$S/V = CL^x. \quad (26)$$

Fitting the data of table 2 to this law, discarding the results from  $L < 24$  yields  $S/V = 1.008(4)L^{-0.527(1)}$  ( $\chi^2/\text{dof}=0.4$ ). The integrated autocorrela-

tion times of the energy, the susceptibility, and of the  $Z_a/Z_p$  measurements (see below) were also fitted to power laws,  $\tau = cL^z$ , using data from all lattice sizes. Only for  $\tau_b$  the  $L = 6$  data were discarded. The fit results are summarized in the following table:

|             | $c$     | $z$       | $\chi^2/\text{dof}$ |
|-------------|---------|-----------|---------------------|
| $\tau_E$    | 1.04(2) | 0.035(7)  | 0.90                |
| $\tau_\chi$ | 1.30(3) | -0.044(7) | 0.57                |
| $\tau_b$    | 0.60(2) | -0.028(8) | 0.71                |

These numbers should be compared with the corresponding ones from the single cluster algorithm [15]:

| $L$ | $\tau_E$ | $\tau_\chi$ |
|-----|----------|-------------|
| 16  | 1.36(2)  | 1.01(2)     |
| 24  | 1.50(3)  | 1.06(2)     |
| 32  | 1.72(4)  | 1.14(3)     |
| 48  | 1.90(6)  | 1.20(4)     |
| 64  | 1.97(5)  | 1.20(3)     |

These  $\tau$ 's are fitted by  $\tau_E \propto L^{0.28(2)}$  and  $\tau_\chi \propto L^{0.14(2)}$ . We conclude that the exponents  $z$  of the wall algorithm are smaller than those of the single cluster algorithm. For the lattice sizes in question, however, the actual  $\tau$ 's are of similar size.

For the measurements of  $Z_a/Z_p$  we employed a variant of the boundary flip algorithm [16], where the cluster that has been built is not flipped but used to construct an observable.

For details on the statistics and lattice sizes of all the runs, see table 3. The total CPU consumption of the standard action runs was about 1.1 years on a 200 MHz Pentium Pro PC for the wall cluster simulations. All simulations with the demon algorithm for the standard Ising model took about half a year on a 200 MHz Pentium Pro PC.

## 3.2 Improved Action

A first estimate for  $\beta_c$  was obtained by locating the crossings of  $R_i(L)$  with  $R_i(2L)$ . We used lattices of size  $L = 4, 8, 16, 32$  and obtained  $\beta_c =$

| Standard Action |           |     |           | Improved Action       |         |              |
|-----------------|-----------|-----|-----------|-----------------------|---------|--------------|
| Cluster         |           |     | Multispin |                       | Cluster |              |
| $L$             | stat/3000 | $k$ | $L$       | stat/ $32 \cdot 10^6$ | $L$     | stat/ $10^6$ |
| 4               | 100000    | 4   | 2         | 200                   | 4       | 30           |
| 6               | 100000    | 4   | 3         | 200                   | 6       | 60           |
| 8               | 100000    | 4   | 4         | 200                   | 8       | 36           |
| 10              | 50100     | 4   | 5         | 200                   | 10      | 10           |
| 12              | 33000     | 7   | 6         | 200                   | 12      | 10           |
| 14              | 25911     | 4   | 7         | 195                   | 14      | 10           |
| 16              | 18207     | 7   | 8         | 155                   | 16      | 13           |
| 20              | 10950     | 4   | 9         | 120                   | 18      | 8            |
| 24              | 9094      | 7   | 10        | 105                   | 20      | 3            |
| 28              | 7504      | 7   | 11        | 105                   | 22      | 7            |
| 32              | 4811      | 7   | 12        | 100                   | 24      | 3            |
| 40              | 3105      | 7   | 13        | 56                    | 28      | 6            |
| 48              | 2620      | 7   | 14        | 51                    | 32      | 6            |
| 56              | 1501      | 7   | 15        | 50                    | 36      | 5            |
| 64              | 1536      | 7   | 16        | 50                    | 40      | 7            |
| 80              | 703       | 7   | 17        | 50                    | 48      | 5            |
| 96              | 506       | 10  | 18        | 44                    | 56      | 2            |
| 112             | 205       | 10  | 19        | 44                    |         |              |
| 128             | 203       | 10  |           |                       |         |              |

Table 3: Left part of table: Statistics of the runs with standard action at  $\beta = 0.2216545$ . stat denotes the number of measurements. Two measurements were always separated by  $k$  updates with the wall cluster algorithm. Middle: Statistics of the multispin-coding runs. Per measurement the demons are once refreshed canonically, and there are 8 microcanonical updates of the spin-system. Last two columns: Number of measurements at  $(\beta, D) = (0.383245, 0.624235)$  in case of the spin-1 model. Two measurements were separated by three cluster updates and one Metropolis sweep.

0.383245(10), with  $D$  given by eq. (24), i.e.  $D_c = 0.624235$ . Note that this was still a preliminary estimate to be refined later.

Monte Carlo simulations were then performed at  $\beta = 0.383245$ , fixing  $D$  according to eq. (24). We simulated on cubic lattices with linear extension  $L$  ranging from 4 to 56, using the single cluster algorithm in alternation with a Metropolis procedure to maintain ergodicity. Two measurements were separated by three single cluster updates and one Metropolis sweep. As for the standard action we used clusters built with the boundary flip algorithm to obtain estimates for  $Z_a/Z_p$ . After each growth of the corresponding cluster, the work done was also exploited to perform one wall cluster step as described for the standard action above. More detailed information on the lattice sizes and the statistics can be obtained from table 3.

The runs for the determination of  $\beta_c$  took about three months of CPU on Pentium 166-MMX PCs, while the final production runs consumed a total of one year CPU on the same type of PC.

## 4 Measured Quantities and Basic Data

The estimates for the basic quantities relevant for the present study are quoted in a number of tables in the Appendix. Here is an overview:

| quantities   | model           | table |
|--|-----------------|-------|
| $R_1, R_2, \chi, E_{NN}$   | Standard Action | 25    |
| $R_1, R_2, \chi$   | Improved Action | 26    |
| $E_{NN}, E_D, E$   | Improved Action | 27    |
| $dR_1/d\beta, dR_2/d\beta$   | Standard Action | 28    |
| $\partial R_1/\partial\beta, dR_1/d\beta, \partial R_2/\partial\beta, dR_2/d\beta$ | Improved Action | 29    |

In both models we measured  $R_1, R_2$ , which were already defined in eqs. (5) and (6). We also measured the quantities needed to estimate the derivatives of  $R_1$  and  $R_2$  with respect to the couplings. Note that in case of the spin-1 model, eq. (24) implies that

$$\frac{dR_i}{d\beta} = \frac{\partial R_i}{\partial\beta} + 3 \frac{\partial R_i}{\partial D}. \quad (27)$$

For the sake of table presentation, the derivatives of the  $R_i$  were multiplied by a factor  $f(L) = L^{-1/0.63}$ , which compensates for the leading divergent be-

haviour with increasing lattice size. The susceptibilities are defined through

$$\chi = L^3 \langle m^2 \rangle, \quad (28)$$

with  $m$  being the normalized magnetization, cf. eq. (7). In the tables, the susceptibilities are multiplied by a factor  $1/L^2$ . For the standard action we measured the energy per link,

$$E_{NN} = \frac{1}{3L^3} \sum_{\langle i,j \rangle} s_i s_j. \quad (29)$$

The same quantity was measured also for the spin-1 model. Here in addition we determined estimates for

$$E_D = \frac{1}{L^3} \sum_i s_i^2, \quad (30)$$

and

$$E = -3(E_{NN} - E_D). \quad (31)$$

The definition of the energy  $E$  is such that it is proportional to  $\frac{d}{d\beta} \ln Z$ , where the relation of  $\beta$  and  $D$  is given by eq. (24).

Standard reweighting techniques allow us to access the same set of observables in some neighbourhood of the simulation point.

## 5 Fitting the Data

Our aim is to test the improvement which can be reached in the estimates for the phenomenological couplings  $R_i$  and the critical exponents using the improved spin-1 action instead of the standard action. We shall first describe our general approach to the data analysis.

We shall present results obtained from fitting our data for the standard action and the improved spin-1 action to various finite size scaling laws. It will turn out that the estimates obtained from the standard action are always compatible with those extracted from the improved action.

In order to get a first impression of the degree of improvement that can be obtained, the reader is invited to look directly at the tables of the Appendix (table 25 to table 29). One can easily verify the impressively different behaviour of the standard and improved data, respectively.

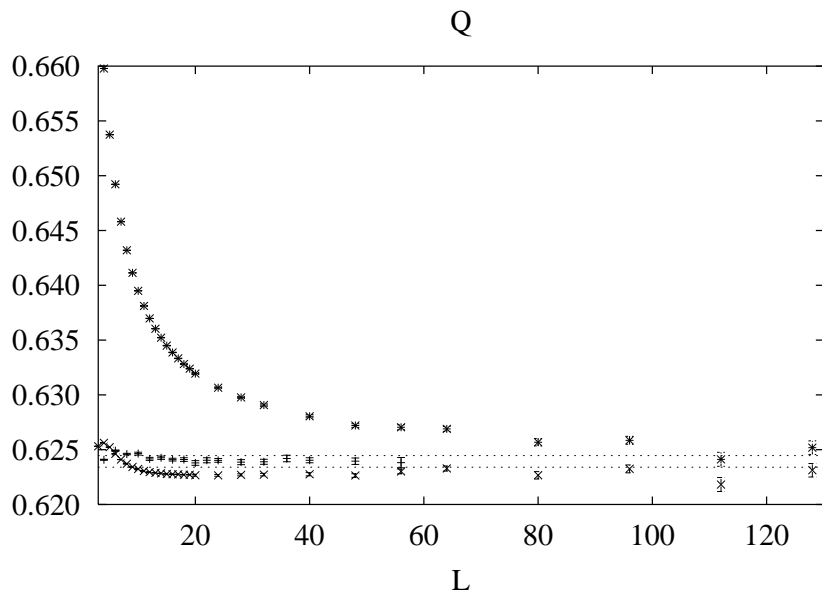


Figure 1:  $R_2 = Q$  as function of lattice size for both models. The upper data (stars) are from the standard action. The bars (flat data) belong to the improved action. Crosses are used to show standard action results corrected with the leading correction to scaling contribution. The final estimate obtained from the fit analysis is plotted by dotted lines.

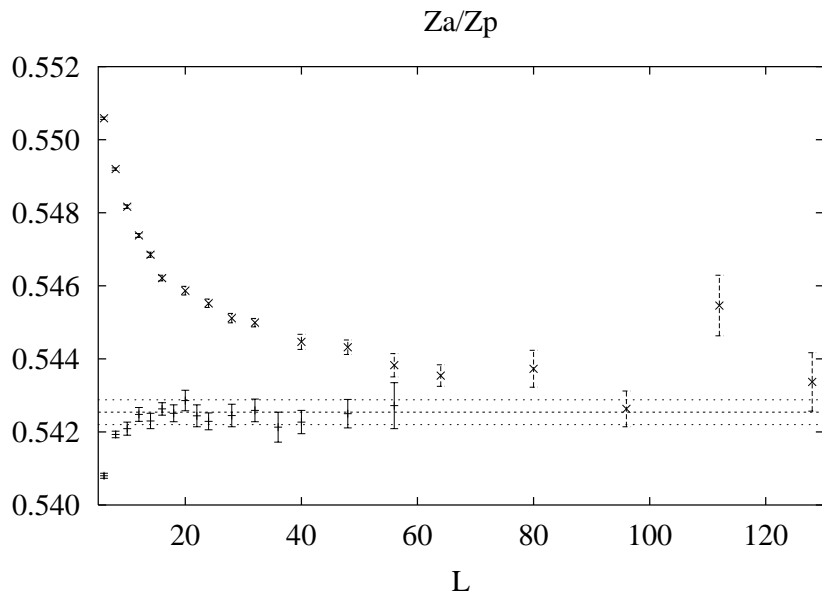


Figure 2:  $R_1 = Z_a/Z_p$  as function of lattice size for both models. Standard action: crosses, improved action: bars. The final estimate obtained from our fit analysis is also plotted with an error interval.

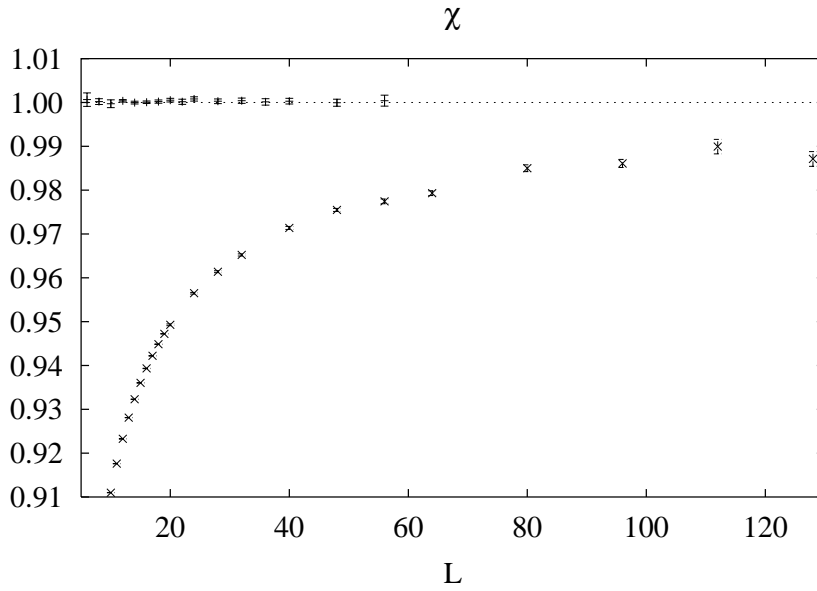
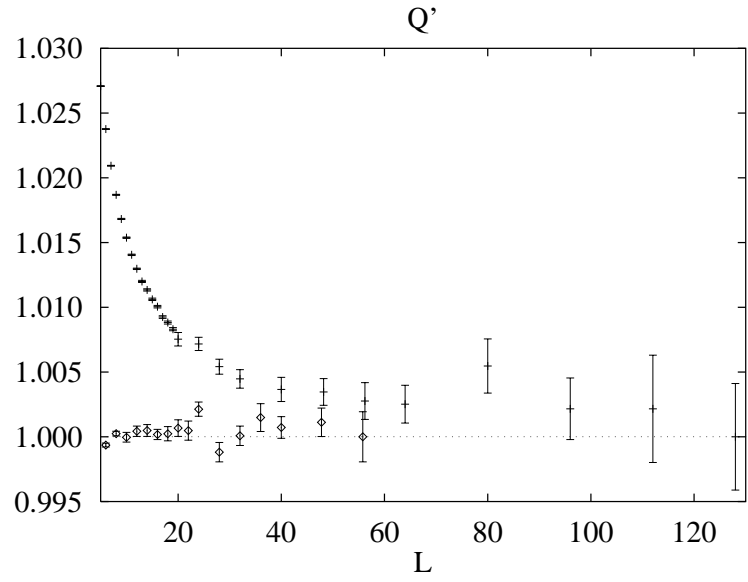


Figure 3: Rescaled  $\beta$  derivatives of  $Q$  and rescaled  $\chi$  at fixed  $Q$  as function of lattice size for both models (see text).

In figure 1, the Binder cumulants  $Q$  are plotted for the two actions, while in figure 2 the critical ratios  $Z_a/Z_p$  are given (tables 25 and 26).

In both figures, the final values obtained from our fit analysis are also given, together with error lines indicating the range of the estimated statistical plus the systematic error. Clearly the improved samples are much more stable and reach their asymptotic regime for very small lattice sizes, while the standard samples hardly get there on lattice sizes of order  $10^2$ . In figure 1 we have in addition plotted the standard action result with the contribution of the leading order correction to scaling subtracted, namely  $Q - 0.105 L^{-0.81}$ , see table 6.

The improved action data outperform the corrected standard action data. This is due to the fact that our improvement procedure not only eliminates correction terms of the form  $L^{-\omega}$ , but also higher order corrections of the form  $L^{-n\omega}$ ,  $n$  integer, which are generated by the same scaling field. In particular corrections of the type  $L^{-2\omega}$  should be present in the observables of the standard Ising model. Interestingly, the corresponding corrections have not been taken into account e.g. in the analysis by Blöte et al. [6], in spite of the fact that  $2\omega$  is smaller than other exponents taken into account in the fit ansätze.

Because of their importance in extracting the critical exponents  $\nu$  and  $\eta$ , in figure 3 we give also the derivatives of  $Q$  and the susceptibilities  $\chi$ . In order to check for a residual  $L$ -dependence and to be able to compare the samples of the two models, the data have been rescaled.

The  $Q$ -derivatives have been multiplied by a factor  $L^{-1/0.63}$  (see tables 28 and 29) and normalized to their value at  $L = 56$  and  $L = 128$ , respectively, for the improved and standard action.

Anticipating some results which will be given below, the  $\chi$ 's have been transformed by  $\chi \rightarrow (\chi - c) L^{\eta-2} d^{-1}$ , where  $c$ ,  $\eta$ , and  $d$  are fit parameters. The values of the various amplitudes were taken from tables 17 and 19.

The authors of ref. [8, 9] claim that the apparent improvement in the scaling behaviour that we demonstrated above does not lead to reduced errors in final results for critical exponents. Taking the data of the improved model by itself they are in fact right. Since the coupling parameters of the model are determined numerically one has to expect some small residual  $L^{-\omega}$  corrections, which lead to systematic errors when not taken into account in the fit ansätze.

However, we shall demonstrate that it is well possible to estimate the effects of residual corrections to scaling in a systematic way. We shall exploit

the fact that ratios of correction to scaling amplitudes are universal. Given the parametrization

$$R_i(L) = R_i^* + r_i L^{-\omega} + \dots, \quad (32)$$

and

$$\frac{dR_i}{d\beta} = c_i L^{1/\nu} (1 + b_i L^{-\omega} + \dots), \quad (33)$$

the ratios  $r_i/r_j$  and  $b_i/r_j$  are universal, i.e., do not depend on the details of the models chosen [17]. In particular, they are the same for the standard and improved action. These ratios can be obtained from the analysis of the standard Ising model data and then used in order to estimate the residual correction to scaling amplitudes in the improved action results.

## 5.1 $R_2$ at fixed $R_1$

Analysing the standard model data, it turns out that the Binder cumulant  $Q$  evaluated at a fixed value of  $Z_a/Z_p$  is the optimal (at least concerning the observables that we measured) quantity to detect corrections to scaling.<sup>†</sup> Optimal means here that the relative statistical error of the leading correction to scaling amplitude is the smallest. We computed  $Q$  at  $Z_a/Z_p = 0.5425$ . This means that first the  $\beta(L)$  is computed where  $Z_a/Z_p$  takes the value 0.5425. Then  $Q$  is computed for these  $\beta(L)$ . In the following we use  $\bar{Q}$  to denote this quantity. In principle  $Z_a/Z_p$  could be fixed to any value, however for practical reasons it is preferable to take a good approximation of  $(Z_a/Z_p)^*$ . To leading order  $\bar{Q}$  should behave as

$$\bar{Q} = Q^* + rL^{-\omega} + \dots. \quad (34)$$

First we fitted the data obtained with the improved action. We used as input  $\omega = 0.81$  from ref. [11]. The results are given in table 4. We see that there is still a small amplitude for corrections to scaling present in the data. The value of  $D$  where the leading order corrections to scaling exactly vanish should be slightly larger than the one used in this study.

In order to quantify the improvement that is achieved we have to compare with the data from the standard Ising model. To obtain a consistent result of  $Q^*$  from small lattices we had to include a subleading correction to scaling term  $r' L^{-2\omega}$  in the ansatz. The results are given in table 5.

---

<sup>†</sup>Doing finite size scaling with quantities taken at  $\beta$ -values where a phenomenological coupling is kept to a fixed value is inspired by ref. [18].

**Improved Action**

| $L_{\min}$ | $Q^*$       | $r$        | $\chi^2/\text{dof}$ |
|------------|-------------|------------|---------------------|
| 6          | 0.62369(13) | 0.0039(10) | 1.16                |
| 8          | 0.62369(12) | 0.0040(11) | 1.24                |
| 10         | 0.62362(14) | 0.0047(13) | 1.29                |
| 12         | 0.62371(16) | 0.0036(16) | 0.50                |

Table 4: Fit of  $\bar{Q}$  with correction to scaling term

**Standard Action**

| $L_{\min}$ | $Q^*$       | $r$        | $r'$       | $\chi^2/\text{dof}$ |
|------------|-------------|------------|------------|---------------------|
| 6          | 0.62294(8)  | 0.1191(11) | 0.0574(33) | 1.73                |
| 8          | 0.62326(12) | 0.1131(19) | 0.0825(67) | 0.76                |
| 10         | 0.62343(14) | 0.1092(27) | 0.102(12)  | 0.60                |
| 12         | 0.62329(18) | 0.1128(43) | 0.081(24)  | 0.56                |

Table 5: Fit of  $\bar{Q}$  with correction to scaling terms

Starting from  $L_{\min} = 8$  the fits have a small  $\chi^2/\text{dof}$ . The result for  $Q^*$  obtained from  $L_{\min} = 10$  is consistent with the results from the improved action. There is a clear signal for the leading order corrections to scaling. The corresponding amplitude is stable when  $L_{\min}$  is varied. Also subleading corrections are well visible.

Concerning the comparison of the two models we conclude that leading corrections to scaling in the improved model are reduced by a factor of about  $0.11/0.004 = 28$  compared with the standard Ising model. In order to compute systematic errors due to neglecting  $L^{-\omega}$  corrections in the analysis of the data obtained from the improved model we assume (taking into account the errors in the amplitudes) that leading corrections to scaling are reduced at least by a factor of 22 compared with the standard Ising model. The reduction from 28 to 22 takes into account that we know the ratio of the  $r$ 's only up to some statistical error.

Using the universality of ratios of corrections to scaling amplitudes this reduction has to be the same for all quantities. Hence we can take the correction amplitudes obtained from the standard action and divide it by 22 to obtain a bound on the leading order corrections that are to be expected

**Standard Action**

| $L_{\min}$ | $R_1^*$          | $\beta_c$           | $r_1$      | $\chi^2/\text{dof}$ |
|------------|------------------|---------------------|------------|---------------------|
| 10         | 0.54275(14){49}  | 0.22165446(16){21}  | 0.0347(10) | 1.81                |
| 14         | 0.54304(23){44}  | 0.22165431(19){15}* | 0.0318(22) | 1.88                |
| 16         | 0.54334(26){27}* | 0.22165417(18){11}  | 0.0281(26) | 1.69                |
| 20         | 0.54269(40){24}  | 0.22165443(21){7}   | 0.0369(50) | 1.43                |

| $L_{\min}$ | $R_2^*$          | $\beta_c$           | $r_2$       | $\chi^2/\text{dof}$ |
|------------|------------------|---------------------|-------------|---------------------|
| 12         | 0.62201(6){79}   | 0.22165363(16){64}  | 0.11166(44) | 1.30                |
| 16         | 0.62244(16){40}  | 0.22165405(23){25}* | 0.1077(15)  | 1.01                |
| 20         | 0.62292(31){21}* | 0.22165440(28){9}   | 0.1017(38)  | 1.09                |
| 28         | 0.62321(61){12}  | 0.22165457(40){4}   | 0.0973(87)  | 1.33                |

Table 6: Fitting separately the  $R_i$  with eq. (35), fixing  $\omega = 0.81$ .

in the case of the improved model.

## 5.2 Fitting $R_1$ and $R_2$

We first fitted the  $R_i$  in order to obtain estimates for the phenomenological couplings  $R_i^*$ , and, in addition, for the critical coupling  $\beta_c$ . Here and in the following we use as an estimate of the leading correction to scaling exponent  $\omega = 0.81(2)$  from ref. [11].

### 5.2.1 Standard Action, Fit $R_i$

In the case of the standard action we fitted our data with the ansatz

$$R_i(L, \beta_{MC}) = R_i^* + \frac{dR_i}{d\beta}(L, \beta_{MC}) \Delta\beta + r_i L^{-\omega}. \quad (35)$$

In addition to a correction to scaling term of the form  $r_i L^{-\omega}$  we included a term which (to first order) corrects for deviations from being at criticality.  $\Delta\beta$  is the difference between the critical  $\beta_c$  and  $\beta = 0.2216545$ . Fitting  $R_1$  to this law, we first fixed  $\omega = 0.81$ . The fits were done on a sequence of data sets obtained by discarding data with  $L < L_{\min}$ . The results for the fit parameters as function of the smallest lattice size included are given in table 6. The procedure used to compute the estimates of the systematic

**Standard Action**

| $L_{\min}$ | $R_2^*$      | $r_2$       | $\omega$   | $\beta_c$      | $\chi^2/\text{dof}$ |
|------------|--------------|-------------|------------|----------------|---------------------|
| 6          | 0.623670(82) | 0.13732(51) | 0.9384(37) | 0.22165434(19) | 2.60                |
| 8          | 0.62433(14)  | 0.1449(18)  | 0.9802(93) | 0.22165489(21) | 0.89                |
| 10         | 0.62455(22)  | 0.1490(40)  | 0.998(18)  | 0.22165503(22) | 0.94                |
| 16         | 0.62494(77)  | 0.174(20)   | 1.070(77)  | 0.22165515(43) | 0.92                |
| 20         | 0.6252(22)   | 0.22(11)    | 1.16(25)   | 0.22165517(61) | 1.12                |

Table 7: Fit of  $R_2$  with eq. (35).

errors (curly brackets) is discussed at the end of this section. In the table we mark with an asterisk the value of  $L_{\min}$  where the systematic error estimate becomes equal or smaller than the statistical estimate.

The fits are reasonably stable. Figure 4 shows the fit results for  $R_1^*$  and  $\beta_c$  as function of  $L_{\min}$ . In addition, the figure gives an impression on the dependence of the estimates on the choice of the fixed  $\omega$ , by varying its value through 0.78 to 0.83. The conclusion is that the dependence on the choice of  $\omega$  is negligible compared to the statistical errors and the systematic errors quoted in table 6. Note that here and in the following all error ranges for final fit results in the plots (usually indicated by a set of horizontal lines) are obtained by *adding* the statistical and systematic errors.

Let us now turn to the cumulant  $R_2$ . The results are given in table 6 and in figure 5. In the figure also the results of table 7, where we have let  $\omega$  a free parameter, are shown. The outcome of  $\omega$  is significantly larger than 0.81, which we presently accept as a reliable estimate. We interpret this as a sign that this fit parameter tries to compensate for the lack of even higher correction exponents.

We also fitted the two  $R_i$  together. We did this by allowing  $\omega$  to vary freely. For  $R_1$ , the exponent  $\omega$  is the only correction to scaling, whereas for  $R_2$  we included additionally a correction term with exponent  $x$ . We checked the two possibilities to either fix the exponent  $x$  to some value or subject it to fitting in order to assume some effective value. Indeed, beyond the leading correction to scaling exponent  $\omega$ , there are several exponents that could enter the game, like for instance  $2\omega$ ,  $x \approx 2$ , or  $1/\nu + \omega$ . In table 8 we present the fit results.

Notice that the amplitude of the leading correction to scaling is much smaller for  $R_1$ , as expected, and for  $R_2$  also the amplitude of the next-

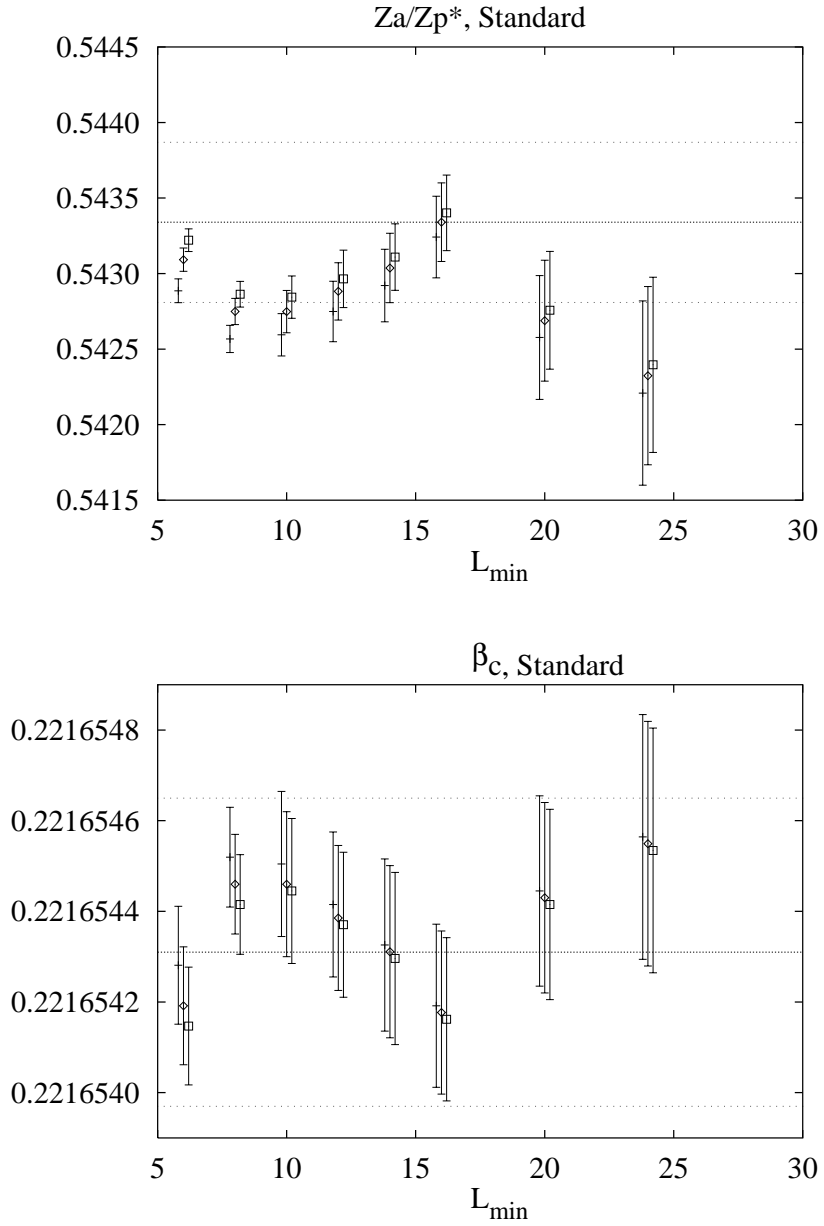


Figure 4:  $R_1^*$  and  $\beta_c$ , standard action, from fits to eq. (35), with fixed exponents  $\omega = 0.78, 0.81, 0.83$ .

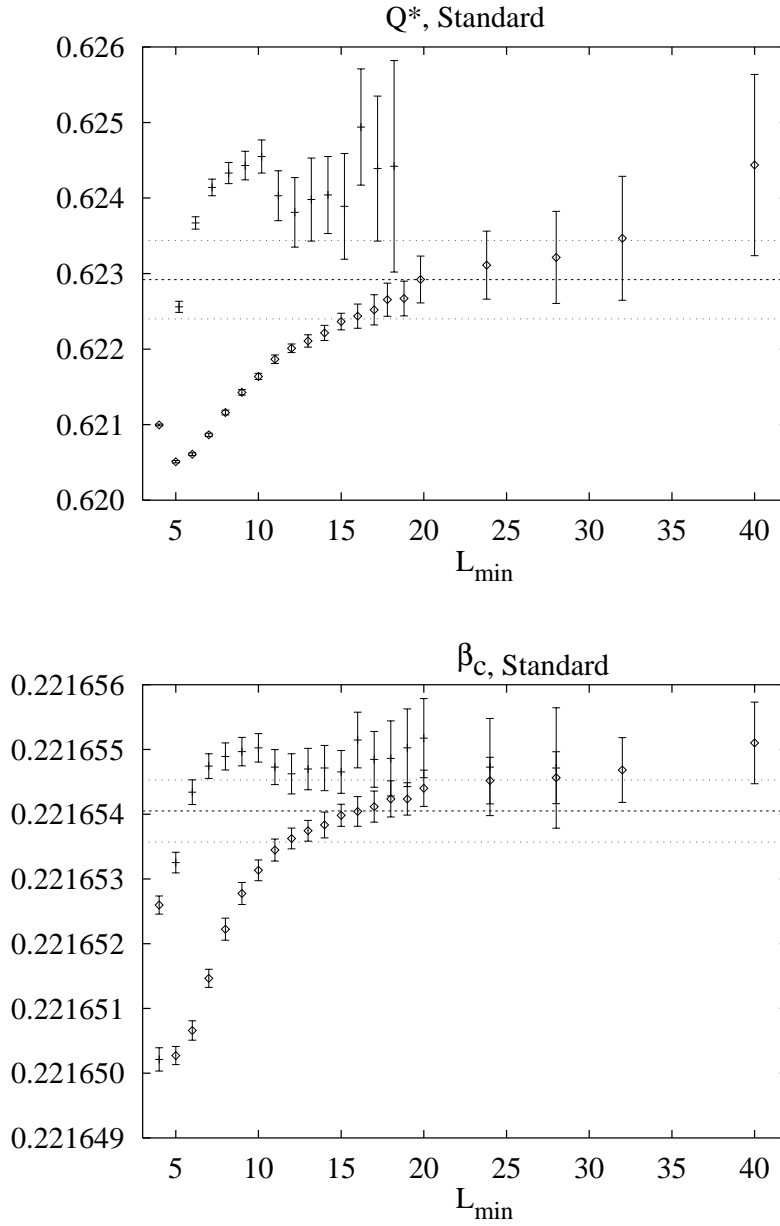


Figure 5:  $R_2^*$  and  $\beta_c$ , standard action, from fits with eq. (35). Diamonds:  $\omega = 0.81$  fixed. Bars:  $\omega$  free fit parameter.

### Standard Action

| $x$      | $R_1^*$         | $R_2^*$         | $\beta_c$          | $\omega$  |
|----------|-----------------|-----------------|--------------------|-----------|
| 1.62     | 0.54120(19)     | 0.62295(25)     | 0.22165516(11)     | 0.670(37) |
| 2.0      | 0.54256(15)     | 0.62261(25)     | 0.22165443(11)     | 0.772(31) |
| 2.4      | 0.54305(13)     | 0.62325(24)     | 0.22165437(11)     | 0.865(27) |
| 2.30(41) | 0.54285(31)     | 0.62261(29)     | 0.22165428(14)     | 0.800(58) |
| final    | 0.54334(26){27} | 0.62292(31){21} | 0.22165431(19){15} |           |

| $x$      | $r_1$      | $r_2$      | $r'_2$    | $\chi^2/\text{dof}$ |
|----------|------------|------------|-----------|---------------------|
| 1.62     | 0.0324(20) | 0.058(11)  | 0.168(19) | 4.40                |
| 2.0      | 0.0330(19) | 0.0907(87) | 0.152(25) | 1.60                |
| 2.4      | 0.0373(17) | 0.1151(72) | 0.136(36) | 1.31                |
| 2.30(41) | 0.0334(28) | 0.100(32)  | 0.184(25) | 1.63                |

Table 8: Fitting together  $R_1$  and  $R_2$  for  $L_{\min} = 8$ . For  $R_1$  we used eq. (35), while for  $R_2$  also an effective next-to-leading correction  $r'_2 L^{-x}$  was added.

to-leading correction to scaling  $r'_2$  is significantly different from zero. The effective next-to-leading exponent is of order two, and actually compatible with that appearing in the improved case. This could well be a coincidence.

Finally, the errors of this fit are smaller than the (safer) errors obtained from the fits with fixed  $\omega$ . However, as a consequence of the limited number of lattice sizes available, the fit with many parameters can not be checked for stability with respect to varying  $L_{\min}$ .

In order to get a handle on the systematic errors due to the neglect of higher order corrections, we used the result from the previous simultaneous fit of  $R_1$  and  $R_2$  to estimate the effective next-to-leading exponents. We assume this exponent  $x$  to be of order 2. Notice that from table 8 it turns out that the value of  $r'_2$  does not depend strongly on  $x$ . The same holds for  $r'_1$ , which is estimated to be of order 0.02 by a 4-parameter fit with  $\omega = 0.81$ ,  $x = 2.3$ , on  $Z_a/Z_p$ .

Then we fitted separately to eq. (35) the quantities defined by

$$\tilde{R}_i(L) = R_i(L) - r'_i L^{-x}, \quad (36)$$

where  $R_i(L)$  are the original (Monte Carlo) data, and  $r'_i$  and  $x$  have fixed values determined by the fits discussed above, namely  $r'_1 = 0.02$ ,  $r'_2 = 0.184$ ,

and  $x = 2.3$ .

Roughly speaking, the  $\tilde{R}_i(L)$  are the original data after subtraction of an estimate of the subleading correction to scaling contamination.

The absolute values of the differences between the  $R_i^*$  and  $\beta_c$  obtained in this way and those obtained from fitting  $R_i(L)$  with the same equation are the estimates of the systematic errors given (inside curly brackets) in table 6.

In summary, from table 6 we obtain the following final estimates (labelled with a \* in the table):

$$\begin{aligned}
 R_1^* &= 0.54334(26)\{27\} \\
 \text{standard action: } R_2^* &= 0.62292(31)\{21\} \\
 \beta_c &= 0.22165431(19)\{15\} \text{ from } R_1 \\
 \beta_c &= 0.22165405(23)\{25\} \text{ from } R_2
 \end{aligned}$$

The final estimates together with their error-lines are also given in figures 4 and 5.

### 5.2.2 Improved Action, Fit $R_i$

We fitted the data to

$$R_i(L, \beta_{\text{MC}}) = R_i^* + \frac{dR_i}{d\beta}(L, \beta_{\text{MC}}) \Delta\beta. \quad (37)$$

Again we included a term which (to first order) corrects for deviations from being at criticality.  $\beta_{\text{MC}}$  is our simulation coupling 0.383245, and the  $dR_i/d\beta$  are taken from table 29. The fit parameters are  $R_i^*$  and  $\beta_c$ , entering through  $\Delta\beta = \beta_{\text{MC}} - \beta_c$ . We first fitted separately  $R_1$  and  $R_2$  in order to compare their scaling behaviour. The results are reported in table 9. For both quantities the fit parameter estimates are quite stable.

Here and in the following, for what concerns estimates obtained from the improved action, in addition to the usual error bars (quoted in usual brackets), we quote for each fit parameter two systematic errors. The systematic errors are meant as an estimate of the uncertainty due to corrections to scaling terms. The first one, square brackets, estimates the error made neglecting a leading correction scaling term. The second one, curly brackets, as in the standard action case, estimates the error made neglecting higher subleading corrections to scaling. They were obtained in a well defined way to be described at the end of this section.

**Improved Action**

| $L_{\min}$ | $R_1^*$              | $\beta_c$           | $\chi^2/\text{dof}$ |
|------------|----------------------|---------------------|---------------------|
| 8          | 0.54213(8) [24]{66}  | 0.3832470(8)[8]{36} | 1.78                |
| 10         | 0.54240(10)[19]{32}  | 0.3832453(9)[5]{15} | 0.79                |
| 12         | 0.54251(11)[17]{21}  | 0.3832447(9)[4]{9}* | 0.49                |
| 16         | 0.54260(15)[16]{15}* | 0.3832442(11)[4]{5} | 0.46                |
| 20         | 0.54252(25)[13]{10}  | 0.3832446(14)[2]{3} | 0.55                |

| $L_{\min}$ | $R_2^*$            | $\beta_c$             | $\chi^2/\text{dof}$ |
|------------|--------------------|-----------------------|---------------------|
| 8          | 0.62447(6)[76]{30} | 0.3832499(10)[46]{29} | 2.22                |
| 10         | 0.62429(7)[62]{15} | 0.3832479(12)[31]{12} | 1.39                |
| 12         | 0.62414(8)[57]{11} | 0.3832465(11)[26]{9}  | 0.42                |
| 16         | 0.62405(12)[50]{7} | 0.3832457(14)[20]{5}  | 0.31                |
| 20         | 0.62393(18)[43]{4} | 0.3832447(18)[17]{3}* | 0.28                |

Table 9: Fitting separately the  $R_i$  with eq. (37). The numbers in square and curly brackets are estimates of the systematic errors (see text).

**Improved Action**

| $L_{\min}$ | $R_1^*$             | $R_2^*$            | $\beta_c$            | $\chi^2/\text{dof}$ |
|------------|---------------------|--------------------|----------------------|---------------------|
| 8          | 0.54206(7)[11]{65}  | 0.62441(5)[64]{32} | 0.3832481(6)[13]{34} | 2.19                |
| 10         | 0.54231(9)[7]{32}   | 0.62421(6)[51]{16} | 0.3832463(7)[8]{14}  | 1.21                |
| 12         | 0.54245(11)[7]{22}  | 0.62408(7)[46]{11} | 0.3832453(8)[6]{9}   | 0.51                |
| 16         | 0.54254(14)[6]{14}* | 0.62399(8)[40]{7}  | 0.3832448(9)[6]{5}*  | 0.42                |
| 20         | 0.54252(22)[4]{9}   | 0.62393(13)[35]{5} | 0.3832446(11)[4]{3}  | 0.41                |

Table 10: Fitting simultaneously the  $R_i$  with eq. (37).

### Improved Action

| $x$      | $R_1^*$            | $R_2^*$            | $\beta_c$          | $\chi^2/\text{dof}$ |
|----------|--------------------|--------------------|--------------------|---------------------|
| 0.81     | 0.54423(23)        | 0.62314(13)        | 0.383241(1)        | 1.52                |
| 2.0      | 0.54287(12)        | 0.62394(7)         | 0.383244(1)        | 1.00                |
| 2.5      | 0.54268(11)        | 0.62405(7)         | 0.3832446(8)       | 0.96                |
| 2.46(56) | 0.54269(17)        | 0.62405(13)        | 0.3832446(11)      | 1.00                |
| final    | 0.54254(14)[6]{14} | 0.62393(13)[35]{5} | 0.3832448(9)[6]{5} |                     |

| $x$      | $r_1$      | $r_2$     |
|----------|------------|-----------|
| 0.81     | -0.014(1)  | 0.0076(6) |
| 2.0      | -0.07(6)   | 0.036(4)  |
| 2.5      | -0.162(13) | 0.080(8)  |
| 2.46(56) | -0.15(57)  | 0.07(22)  |

Table 11: Fitting simultaneously the  $R_i$  with eq. (38), see text.

We also fitted all the  $R_i$ -data together with three parameters ( $R_1^*$ ,  $R_2^*$ , and  $\beta_c$ ). The results are presented in table 10.

Before describing the procedure we used to estimate systematic errors for the improved action case, let us report the results from a simultaneous fit of  $R_1$  and  $R_2$  with the law

$$R_i(L, \beta_{\text{MC}}) = R_i^* + \frac{dR_i}{d\beta}(L, \beta_{\text{MC}}) \Delta\beta + r_i L^{-x}. \quad (38)$$

As already discussed in the previous section,  $x$  represents an effective exponent.

Our fit results are summarized in table 11. In the first three lines fits with fixed  $x$  are shown, while in the fourth  $x$  is a free parameter. All these fits correspond to  $L_{\text{min}} = 6$ . In the fifth line our final estimates are given for comparison.

If we force the  $x$ -exponent to assume the leading correction value  $\omega = 0.81$ , we observe that  $\chi^2/\text{dof}$  is a little larger than for the other values of  $x$ . The correction amplitudes  $r_i$  are very small. The main problem of this fit is that the ratio  $r_1/r_2$  is completely inconsistent with that found for the standard Ising action.

Leaving  $x$  free, it tends to choose a value around 2.5. However the corresponding fit does not improve on the estimates of the fit without correction

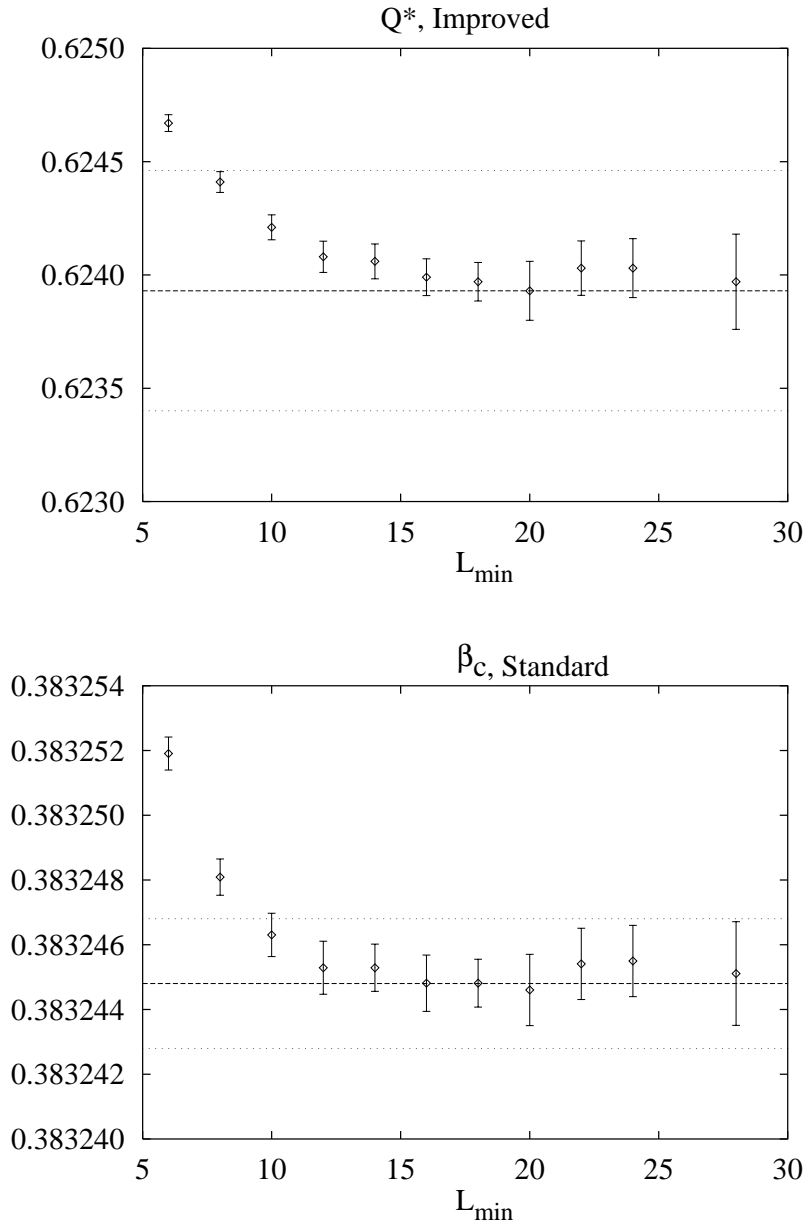


Figure 6:  $R_2^*$  and  $\beta_c$  as function of smallest lattice size included in a common fit of  $R_1$  and  $R_2$  data to eq. (37).

to scaling, though consistent with it. Compare also the fits with  $x$  fixed to 2 and to 2.5.

Note that the  $\chi^2/\text{dof}$  values do not allow to discriminate between the different solutions, i.e. the different exponents. Obtaining estimates from a (relatively) large lattice limit of fits without correction to scaling is, in this case, a safer procedure compared to a multi-parameter fit on all lattice sizes, in principle legitimate but in practice difficult to control.

Being the  $\chi^2/\text{dof}$  not a good signal of the presence of correction to scaling terms, we estimated the systematic error due to neglecting the leading correction to scaling term as well as that due to subleading corrections.

For the estimates of errors due to leading corrections to scaling we used the following procedure (systematically used also in the following sections). From table 6 we know with good precision the leading correction amplitudes  $r_i^{(S)}$  for the standard action. From the universality argument discussed in section 5.1, we assume that the corresponding amplitudes for the improved action are given by  $r_i^{(S)}/22$ . Therefore, analogously to eq. (36), we define the tilde quantities

$$\tilde{R}_i(L) = R_i(L) - \frac{r_i^{(S)}}{22} L^{-\omega} . \quad (39)$$

As in the previous section, fitting  $\tilde{R}_i$  and  $R_i$  with eq. (37) and taking the absolute value of the differences of the outcome parameters gives the estimates reported in square brackets.

The information from the fits of table 11 with the extra exponent  $x$  can instead be used to estimate in a systematic way the effect of ignoring the corresponding corrections. We define again

$$\tilde{R}_i(L) = R_i(L) - r_i L^{-x} , \quad (40)$$

where  $x$  and  $r_i$  are parameters obtained from the fits reported in table 11, namely  $r_1 = 0.07$ ,  $r_2 = -0.15$ , and  $x = 2.46$ . Repeating the steps followed above, one obtains the estimates given in curly brackets.

Using the fit estimates marked with an asterisk, i.e., where statistical and systematic error estimates are of the same order, we obtain our final estimates:

$$\begin{aligned} R_1^* &= 0.54254(14)[6]\{14\} \\ \text{improved action: } R_2^* &= 0.62393(13)[35]\{5\} \\ \beta_c &= 0.3832448(9)[6]\{5\} \end{aligned}$$

### Standard Action

| $L_{\min}$ | $a_1$       | $\nu$            | $\chi^2/\text{dof}$ |
|------------|-------------|------------------|---------------------|
| 10         | -1.4723(7)  | 0.62981(7)[102]  | 5.38                |
| 20         | -1.4798(26) | 0.63045(21)[85]  | 1.00                |
| 28         | -1.4747(36) | 0.63008(27)[69]  | 0.88                |
| 40         | -1.4757(79) | 0.63014(54)[55]* | 0.96                |
| 48         | -1.4699(13) | 0.62977(88)[48]  | 1.09                |

| $L_{\min}$ | $a_2$        | $\nu$           | $\chi^2/\text{dof}$ |
|------------|--------------|-----------------|---------------------|
| 14         | 0.87050 (71) | 0.6331(1)[31]   | 3.35                |
| 24         | 0.8592 (29)  | 0.6315(4)[18]   | 0.66                |
| 40         | 0.8501(76)   | 0.6305(9)[13]   | 0.26                |
| 48         | 0.850(12)    | 0.6304(13)[11]* | 0.31                |
| 56         | 0.848(14)    | 0.6303(15)[11]  | 0.39                |

Table 12: Fitting  $dR_1/d\beta$  (top) and  $dR_2/d\beta$  (bottom) with eq. (41).

The  $R_2^*$  and  $\beta_c$  (as function of  $L_{\min}$ ) are shown in figure 6. In the figures, our final estimates are also indicated by dashed lines, with the error intervals bounded by dotted lines.

## 5.3 Fitting the Derivatives of the $R_i$

### 5.3.1 Standard Action, Fit $dR_i/d\beta$

We first fit the  $dR_i/d\beta$  without correction to scaling,

$$\frac{\partial R_i}{\partial \beta} = a_i L^{1/\nu}. \quad (41)$$

The corresponding results are summarized in table 12. As expected, both quantities suffer from strong corrections to scaling. Let us first estimate the systematic error due to the leading correction. We followed the procedure described in section 5.2. Namely, we made fits with the ansatz

$$\frac{\partial R_i}{\partial \beta} = a_i L^{1/\nu}(1 + b_i L^{-\omega}), \quad (42)$$

**Standard Action**

| $L_{\min}$ | $a_2$      | $\nu$                | $b_2$      | $\chi^2/\text{dof}$ |
|------------|------------|----------------------|------------|---------------------|
| 8          | 0.8418(20) | 0.62999(25){93}<20>  | 0.1103(59) | 0.48                |
| 10         | 0.8396(29) | 0.62973(36){61}<17>  | 0.1181(95) | 0.47                |
| 12         | 0.8395(36) | 0.62973(43){46}<14>* | 0.119(13)  | 0.52                |
| 14         | 0.8333(48) | 0.62908(55){37}<16>  | 0.147(19)  | 0.35                |

Table 13: Fitting  $dR_2/d\beta$  with eq. (42) and fixed  $\omega = 0.81$ .

then we defined

$$\frac{\partial \tilde{R}_i}{\partial \beta} = \frac{\partial R_i}{\partial \beta} - a_i b_i L^{1/\nu - \omega}, \quad (43)$$

and finally we fitted the tilde quantities to eq. (41), fixing  $\omega = 0.81$ . The differences in the  $\nu$  exponents are given in the square brackets of table 12. The leading amplitude corrections  $b_i$  can be found in table 13 and table 14.

The derivative of  $R_2$  suffers from stronger systematic effects than the  $R_1$  derivative. Therefore we include the  $\omega$  correction into the fit ansatz (namely, we fit with eq. (42)) and compute the systematic error made neglecting further subleading correction to scaling. The fit results are given in table 13 and in figure 7, where also the  $\nu$ -exponents obtained from the fit with eq. (41) are reported for comparison.

In the table we have included as a third error bar (in  $\langle \rangle$  brackets) estimates of the systematic effect from varying  $\omega$  from 0.77 through 0.85. This covers a  $2\text{-}\sigma$ -interval around the  $\omega$  value 0.81(2) that we decide to use. Again, the systematic error estimates in curly brackets take into account the omission of next-to-leading corrections to scaling. They were computed with the procedure discussed at the end of section 5.2.1. We fitted with the ansatz

$$\frac{\partial R_i}{\partial \beta} = a_i L^{1/\nu} (1 + b_i L^{-\omega} + b'_i L^{-x}), \quad (44)$$

and defined the tilde quantities subtracting a contribution  $a_2 b'_2 L^{1/\nu - 2}$ , with an estimate  $b'_2 = -0.1$ .

In table 14 we give for comparison the results of fitting  $R_1$  to eq. (44) for  $L_{\min} = 8$ . Notice that in this case the data signals the presence of a stronger next-to-leading correction to scaling. The  $\nu$  obtained in this way is anyhow consistent with the final estimate obtained from the  $R_2$  derivative.

We quote as our final estimates

**Standard Action**

| $x$  | $a_1$      | $\nu$       | $b_1$     | $b'_1$    | $\chi^2/\text{dof}$ |
|------|------------|-------------|-----------|-----------|---------------------|
| 1.62 | -1.446(12) | 0.62873(69) | 0.175(44) | -0.65(11) | 0.94                |
| 2.0  | -1.460(10) | 0.62943(61) | 0.091(32) | -0.83(13) | 1.0                 |
| 2.4  | -1.469(9)  | 0.62993(55) | 0.046(26) | -1.27(20) | 1.1                 |

Table 14: Fitting  $dR_1/d\beta$  with eq. (44) and fixed  $\omega = 0.81$  for  $L_{\min} = 8$ .

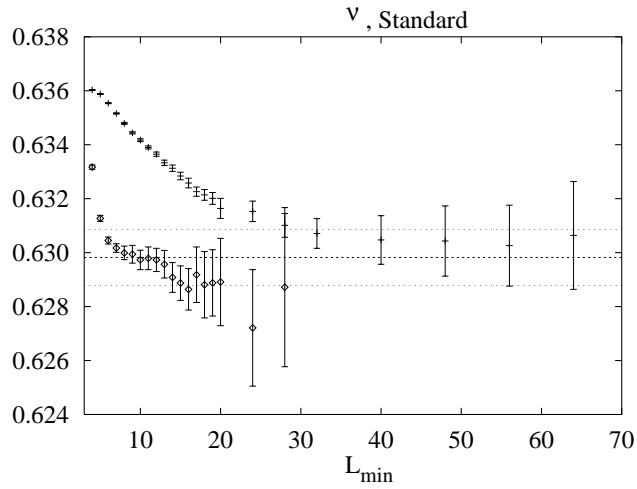


Figure 7:  $\nu$  resulting from fitting  $dR_2/d\beta$ , standard action, without correction to scaling (bars) and with  $\omega = 0.81$  (diamonds).

$$\begin{aligned} \text{standard action: } \nu &= 0.63014(54)[55] && \text{(from table 12)} \\ \nu &= 0.62973(43)\{46\}\langle 14 \rangle && \text{(from table 13)} \end{aligned}$$

### 5.3.2 Improved Action, Fit $\partial R_i/\partial\beta$

We fitted our data for the derivatives of the  $R_i$  with respect to  $\beta$ , according to eq. (41). The results are given in table 15. The  $\nu$ -estimates of this table are plotted in figure 8.

Obviously, the derivatives of the cumulant scale better than those of  $Z_a/Z_p$ : while the cumulant's derivative gives a small  $\chi^2/\text{dof}$  already for  $L_{\min} = 6$ , for the  $R_1$ 's derivative one needs  $L_{\min} = 18$  in order to have a small  $\chi^2/\text{dof}$  and to reach stability of the result. However, also in this case the leading correction to scaling is strongly suppressed. Note that the range of lattice sizes considered here is relatively small: the difference in scaling behaviour is actually due to a bigger amplitude of the next-to-leading correction to scaling, as discussed below.

The systematic error estimates due to neglecting leading order correction to scaling are given, as usual, in square brackets. Their evaluation followed the procedure used in section 5.2.2. We defined the tilde quantities by

$$\frac{\partial \tilde{R}_i}{\partial \beta} = \frac{\partial R_i}{\partial \beta} - a_i \frac{b_i^{(S)}}{22} L^{1/\nu-0.81}, \quad (45)$$

where  $a_i$  are given in table 15 and the leading correction amplitudes  $b_i^{(S)}$  of the standard action are taken from table 13 and table 14. The absolute difference of the  $\nu$  obtained fitting to eq. (41) the tilde and the original Monte Carlo data are the error estimates.

The systematic error estimates due to subleading corrections are given in curly brackets. To estimate them, we used a fit ansatz

$$\frac{\partial R_i}{\partial \beta} = a_i L^{1/\nu} (1 + b_i L^{-x}), \quad (46)$$

and then defined as usual the tilde quantities subtracting  $a_i b_i L^{1/\nu-2}$  from the Monte Carlo data. The amplitudes  $b_i$  are given in table 16. Comparing the fit without correction to scaling of the Monte Carlo and of the tilde data we obtained the estimates given in the curly brackets.

Let us make some comments on the results given in table 16. Including very small lattice sizes, the  $R_1$  derivative's deviations from eq. (41) are strong

### Improved Action

| $L_{\min}$ | $a_1$       | $\nu$                  | $\chi^2/\text{dof}$ |
|------------|-------------|------------------------|---------------------|
| 10         | -1.1419(12) | 0.62850(14) [32] {152} | 3.08                |
| 16         | -1.1487(23) | 0.62924(25) [27] {74}  | 0.90                |
| 20         | -1.1543(39) | 0.62979(39) [26] {43}  | 0.32                |
| 24         | -1.1552(51) | 0.62988(51) [32] {51}* | 0.40                |

| $L_{\min}$ | $a_2$       | $\nu$                  | $\chi^2/\text{dof}$ |
|------------|-------------|------------------------|---------------------|
| 6          | 0.66160(42) | 0.62969(11) [22] {41}  | 0.79                |
| 8          | 0.66247(63) | 0.62987(14) [18] {26}  | 0.57                |
| 10         | 0.6622(11)  | 0.62982(22) [16] {15}* | 0.60                |
| 12         | 0.6626(12)  | 0.62989(24) [24] {11}  | 0.64                |

Table 15: Fit of  $\partial R_1/\partial\beta$  (top) and  $\partial R_2/\partial\beta$  (bottom) with eq. (41).

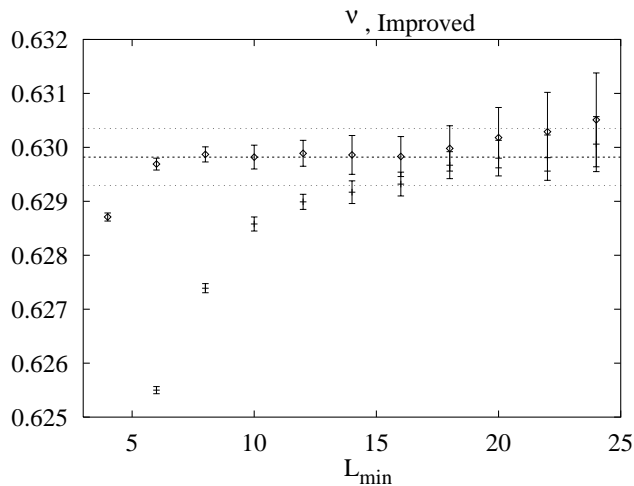


Figure 8: Fit results for  $\nu$  from fitting  $\partial R_i/\partial\beta$ , improved action, with eq. (41). The data with better scaling behaviour belong to  $\partial R_2/\partial\beta$ .

**Improved Action**

| $x$      | $a_1$       | $\nu$       | $b_1$      | $\chi^2/\text{dof}$ |
|----------|-------------|-------------|------------|---------------------|
| 0.81     | -1.20(56)   | 0.63340(46) | -0.163(12) | 0.68                |
| 2.4      | -1.1561(11) | 0.62993(14) | -1.309(31) | 0.34                |
| 2.33(28) | -1.1572(41) | 0.63003(40) | -1.18(68)  | 0.36                |

| $x$ | $a_2$      | $\nu$       | $b_2$      | $\chi^2/\text{dof}$ |
|-----|------------|-------------|------------|---------------------|
| 2.0 | 0.6637(12) | 0.63009(25) | -0.058(29) | 0.63                |
| 2.4 | 0.6635(11) | 0.63005(23) | -0.103(51) | 0.62                |
| 2.8 | 0.6633(10) | 0.63002(21) | -0.190(93) | 0.61                |

Table 16: Fitting  $\partial R_1/\partial\beta$  (top) and  $\partial R_2/\partial\beta$  (bottom) with eq. (46).

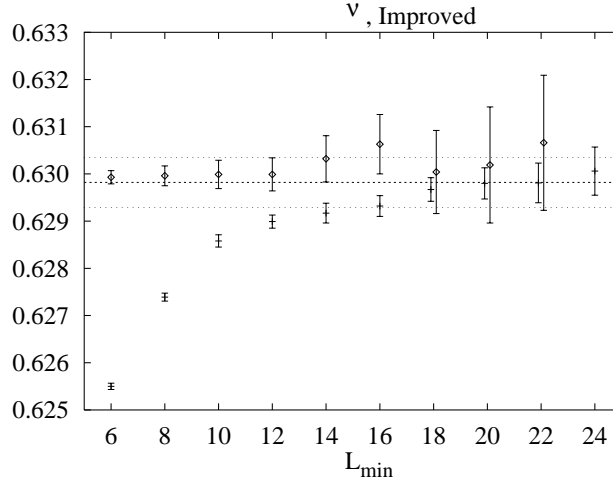


Figure 9: Fits of  $\partial R_1/\partial\beta$ , improved action, with eq. (41) (bars) and with eq. (46) and  $x = 2.4$  fixed (diamonds).

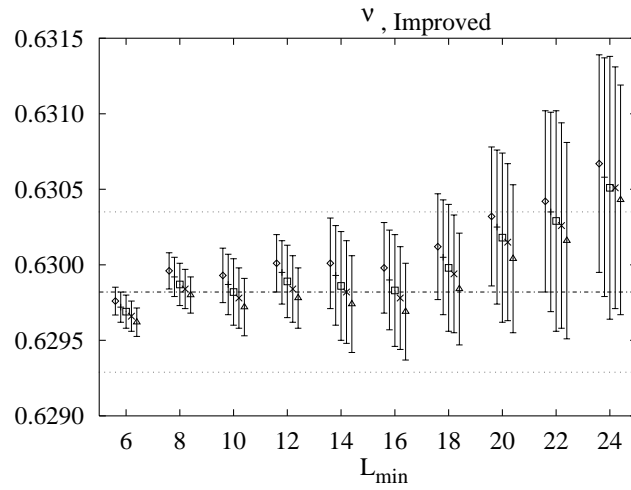


Figure 10: Fit results for  $\nu$  from fitting  $\partial R_2/\partial\beta$ , improved action, with eq. (41). The  $\nu$ -estimate is given for the five  $\beta$ -values 0.383243 to 0.383247 in steps of 0.000001 (left to right).

enough to allow a fit with a free effective exponent, which turns out to be 2.33(28), i.e. again of order 2. Notice again that enforcing  $x = 0.81$  does not prevent the fit from giving an acceptable  $\chi^2$ . We have to rely on the universality of the ratios of correction amplitudes, as discussed before, to rule out this fit.

In figure 9 we plot the fits to  $\partial R_1/\partial\beta$  using eq. (46) for various values of  $L_{\min}$  with fixed exponent  $x = 2.4$ , together with the fits without correction to scaling of table 15. This is sufficient to demonstrate the nice scaling behaviour of the derivative of  $R_1$  once an effective next-to-leading correction to scaling exponent of order 2 has been included in the fit.

In the case of  $\partial R_2/\partial\beta$  the corrections are too small to allow for a free effective exponent fit. Therefore we fix the  $x$ -values between 2.0 and 2.8, as suggested by the fits on  $\partial R_1/\partial\beta$ . The  $\nu$ -results are nicely stable within these bounds and consistent with the values obtained without scaling corrections.

These fits show clearly that the better scaling behaviour of the Binder cumulant derivative is due to a smaller amplitude of the next-to-leading corrections to scaling compared to that of the  $Z_a/Z_p$  derivative.

Finally, we checked also for the systematic dependence on the location of  $\beta_c$  for  $R'_2$ , which is giving the nicest result. We repeated the fits for the  $Q$ -derivative on data from five shifted  $\beta$ -values ranging from 0.383243 to 0.383247 in steps of 0.000001, covering thus two standard deviations around our  $\beta_c$  estimate. The results for  $\nu$  are shown in figure 10. The effects of this variation is negligible compared with the errors of table 15.

We thus quote as our final estimate for  $\nu$

$$\begin{aligned} \text{improved action: } \nu &= 0.62988(51)[32]\{51\} \quad \text{from } \partial R_1/\partial\beta \\ \nu &= 0.62982(22)[16]\{15\} \quad \text{from } \partial R_2/\partial\beta \end{aligned}$$

The final estimate of  $\nu$  appears with dotted error-lines in figures 8, 10 and 9. Recall that to this end the statistical and systematic errors were added up.

## 5.4 Fitting the Susceptibility

### 5.4.1 Standard Action, Fit $\chi$

It turns out that the estimate of  $\eta$  from fits of the magnetic susceptibility  $\chi$  taken at  $\beta_c$  depends quite strongly on the value of  $\beta_c$ . Taking the magnetic susceptibility at a fixed value of a phenomenological coupling removes this problem, as discussed in ref. [18]. One defines a function  $\beta(L)$  by requiring

**Standard Action**

| $L_{\min}$ | $c$        | $d$        | $\eta$      | $f$        | $\chi^2/\text{dof}$ |
|------------|------------|------------|-------------|------------|---------------------|
| 10         | -0.515(83) | 1.5600(44) | 0.03751(62) | -0.585(12) | 0.96                |
| 12         | -0.67(24)  | 1.5548(84) | 0.0368(11)  | -0.568(27) | 0.98                |
| 14         | -1.00(41)  | 1.546(12)  | 0.0358(15)  | -0.537(41) | 1.06                |

Table 17: Fit of  $\chi$  at fixed  $Q = 1/1.604 = 0.62344$ , using eq. (47) with  $\omega = 0.81$ .

**Standard Action**

| $L_{\min}$ | $c$       | $d$       | $\eta$     | $f$        | $\chi^2/\text{dof}$ |
|------------|-----------|-----------|------------|------------|---------------------|
| 8          | -1.08(8)  | 1.543(4)  | 0.0354(5)  | -0.096(12) | 1.22                |
| 10         | -0.78(14) | 1.553(6)  | 0.0366(8)  | -0.130(19) | 1.14                |
| 12         | -1.2(6)   | 1.544(16) | 0.0355(19) | -0.095(61) | 1.15                |
| 14         | -1.5(8)   | 1.538(15) | 0.0348(19) | -0.069(68) | 1.24                |

Table 18: Fit of  $\chi$  at fixed  $Z_a/Z_p = 0.5425$ , using eq. (47) with  $\omega = 0.81$ .

that for any  $L$  the relation  $R_i(L, \beta(L)) = \text{const}$  holds. The susceptibility is then computed at  $\beta(L)$ . We performed this analysis for the two cases of fixing  $Q = 0.6240$  and fixing  $Z_a/Z_p = 0.5425$ . Note that in principle any value for  $Q$  and  $Z_a/Z_p$  that can be taken by the phenomenological couplings would work. However, for practical purposes it is the best to take good approximations of  $R_i^*$ .

We fitted our data to the ansatz:

$$\chi(L, \beta_c(L)) = c + d L^{2-\eta} (1 + f L^{-\omega}), \quad (47)$$

where  $c$  is the leading analytic part of  $\chi$ , and  $f L^{-\omega}$  gives leading order corrections. The results of the fits are given in table 17 and in table 18. In both cases an acceptable  $\chi^2/\text{dof}$  is reached at  $L_{\min} = 10$ . It is interesting to see that the correction to scaling amplitude  $f$  is considerably smaller in the case of fixed  $Z_a/Z_p$ . Therefore it seems reasonable to assume that also  $L^{-2\omega}$  corrections are smaller for fixed  $Z_a/Z_p$ . We thus take  $\eta$  from fixed  $Z_a/Z_p$  at  $L_{\min} = 10$  as our final result. As estimate of the systematic error we quote the difference to the fixed  $Q$  result at  $L_{\min} = 10$ :

$$\text{standard action: } \quad \eta = 0.0366(8)\{9\}.$$

**Improved Action**

| $L_{\min}$ | $c$        | $d$        | $\eta$        | $\chi^2/\text{dof}$ |
|------------|------------|------------|---------------|---------------------|
| 4          | -0.459(8)  | 0.9496(9)  | 0.0351(3)[17] | 0.42                |
| 6          | -0.540(56) | 0.9516(18) | 0.0357(6)[14] | 0.28                |
| 8          | -0.553(77) | 0.9519(20) | 0.0358(6)[14] | 0.30                |
| 10         | -0.58(13)  | 0.9525(29) | 0.0359(9)[12] | 0.32                |
| 12         | -0.55(13)  | 0.9519(28) | 0.0358(8)[12] | 0.33                |

Table 19: Fitting  $\chi$  with eq. (48) at fixed  $Q = 0.6240$ .

**Improved Action**

| $L_{\min}$ | $c$        | $d$        | $\eta$           | $\chi^2/\text{dof}$ |
|------------|------------|------------|------------------|---------------------|
| 4          | -0.541(49) | 0.9545(17) | 0.03664(53)[20]* | 0.15                |
| 6          | -0.538(61) | 0.9544(20) | 0.03662(64)[20]  | 0.15                |
| 8          | -0.532(62) | 0.9543(20) | 0.03657(60)[20]  | 0.15                |
| 10         | -0.511(90) | 0.9538(24) | 0.03644(75)[18]  | 0.15                |
| 12         | -0.53(16)  | 0.9541(32) | 0.03651(94)[16]  | 0.16                |

Table 20: Fitting  $\chi$  with eq. (48) at fixed  $Z_a/Z_p = 0.5425$ .

We have checked that the uncertainty in the estimate of  $\omega$  leads to negligible errors in  $\eta$ . We also performed fits of the magnetic susceptibility without a constant term in the ansatz. It is reassuring that the results for  $\eta$  are consistent with those found above, when  $L_{\min} = 20$  is taken.

#### 5.4.2 Improved Action, Fit $\chi$

Also in the case of the improved action we computed the magnetic susceptibility at fixed  $Q = 0.6240$  and at fixed  $Z_a/Z_p = 0.5425$ . We fitted our data with the ansatz

$$\chi(L, \beta(L)) = c + dL^{2-\eta}. \quad (48)$$

Here we have skipped the term  $L^{-\omega}$ . Our fit results are given in table 19 and plotted in figure 11.

From the Ising model with the standard action we know that the amplitude of the  $L^{-\omega}$  correction is much smaller for  $\chi$  at fixed  $Z_a/Z_p$  than at fixed  $Q$  (see below). Therefore the comparison of both results gives a nice check

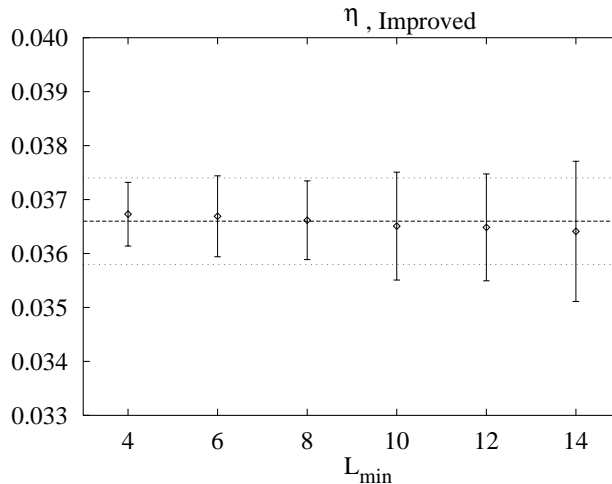


Figure 11:  $\eta$ -estimates, fitting  $\chi$ -data at fixed  $Z_a/Z_p$  to eq. (48), improved action.

of the systematic errors introduced by the omission of a  $L^{-\omega}$  term in the fit ansatz. Since the corrections are smaller in the case of fixed  $Z_a/Z_p$ , we quote the corresponding result as our final estimate.

The systematic error due to the omission of a  $L^{-\omega}$  term in the ansatz is computed in the same way as in the previous sections. Namely, we defined the tilde quantities as

$$\tilde{\chi}(L) = \chi(L) - d \frac{f^{(S)}}{22} L^{2-\eta-0.81}, \quad (49)$$

where  $f^{(S)}$  are taken from table 17 for  $\chi$  at fixed  $Q$  and table 18 for  $\chi$  at fixed  $Z_a/Z_p$ . Then we compare the results obtained fitting the  $\tilde{\chi}$  with eq. (48) and the  $\chi$ , both at fixed  $Q$  and fixed  $Z_a/Z_p$ . The absolute differences of the  $\eta$  obtained in this way are the estimates of the systematic errors. Notice that in this case the next-to-leading correction to scaling enters with an exponent of order 2 which is somehow already taken into account with the analytical contribution denoted by  $c$  in our fit ansätze. Therefore we only quote the systematic error due to the leading correction.

We have chosen the result of  $L_{\min} = 8$  as our final estimate, since it is consistent with the result obtained from  $L_{\min} = 4$  and  $L_{\min} = 6$ . Hence our

final estimate is

$$\text{improved action: } \quad \eta = 0.0366(6)[2].$$

which is consistent with the estimate obtained from the standard action.

## 5.5 Fitting the Energy

As a consistency check we tried to obtain the exponent  $\nu$  from the singular behaviour of the energy. Since it turned out that the statistical errors of the results for  $\nu$  are larger than those obtained from the derivatives of the  $R_i$  we skipped the elaborate analysis of systematic errors that was used above.

### 5.5.1 Improved Action, Fit $E$

The expectation values of the energy  $E$  in the spin-1 model, defined through eq. (31) where subjected to a fit with

$$E = a_E + b_E L^{1/\nu-3}. \quad (50)$$

The results are quoted in table 21. The dependence of the estimate for  $\nu$  on  $L_{\min}$  is shown in figure 12, where the estimates obtained from the standard action are also given.

The results are consistent with the previous estimate of  $\nu$  but with bigger errors. The final  $\nu$ -estimate, with error-lines, obtained from the cumulant derivative for the improved action is plotted for comparison.

### 5.5.2 Standard Action, Fit $E$

We first tried a fit without corrections, using eq. (50). The fit results for the nearest neighbour energy  $E_{NN}$  of the standard action, defined in eq. (29), are given in table 22.

Compared to the case of the improved action, the table starts with much larger  $L_{\min}$ . The corrections to scaling are much bigger than in the improved case. This becomes obvious from a look at figure 12, which shows the dependence of the  $\nu$ -estimate on  $L_{\min}$ . Therefore we take into account corrections to scaling with the ansatz

$$E_{NN} = a_E + b_E L^{1/\nu-3} (1 + c_E L^{-\omega}). \quad (51)$$

The results given in table 23 for  $\omega = 0.81$  show a nice agreement, however with large errors.

**Improved Action**

| $L_{\min}$ | $a_E$       | $b_E$       | $\nu$       | $\chi^2/\text{dof}$ |
|------------|-------------|-------------|-------------|---------------------|
| 6          | 1.23156(14) | -0.9884(18) | 0.62893(39) | 0.58                |
| 10         | 1.23155(23) | -0.9929(64) | 0.6297(11)  | 0.63                |
| 14         | 1.23156(29) | -0.987(11)  | 0.6288(18)  | 0.67                |
| 18         | 1.23157(47) | -0.983(21)  | 0.6281(32)  | 0.77                |

Table 21: Fit of the energy  $E$  with eq. (50).

**Standard Action**

| $L_{\min}$ | $a_E$         | $b_E$      | $\nu$       | $\chi^2/\text{dof}$ |
|------------|---------------|------------|-------------|---------------------|
| 16         | 0.3302003(32) | 0.7331(18) | 0.62902(36) | 0.73                |
| 20         | 0.3302028(47) | 0.7349(39) | 0.62937(72) | 0.75                |
| 28         | 0.3302008(65) | 0.7325(74) | 0.6290(13)  | 0.81                |
| 36         | 0.330201(12)  | 0.733(19)  | 0.6290(30)  | 0.97                |

Table 22: Fit of the energy  $E_{NN}$  with eq. (50).

**Standard Action**

| $L_{\min}$ | $a_E$         | $b_E$      | $\nu$       | $c_E$      | $\chi^2/\text{dof}$ |
|------------|---------------|------------|-------------|------------|---------------------|
| 8          | 0.3302162(32) | 0.7693(35) | 0.63372(53) | -0.155(10) | 1.11                |
| 14         | 0.3302057(59) | 0.754(12)  | 0.6317(16)  | -0.098(44) | 0.87                |
| 18         | 0.3302093(93) | 0.756(30)  | 0.6321(39)  | -0.09(14)  | 0.85                |

Table 23: Fit of the energy  $E_{NN}$  with eq. (51) and  $\omega = 0.81$ .

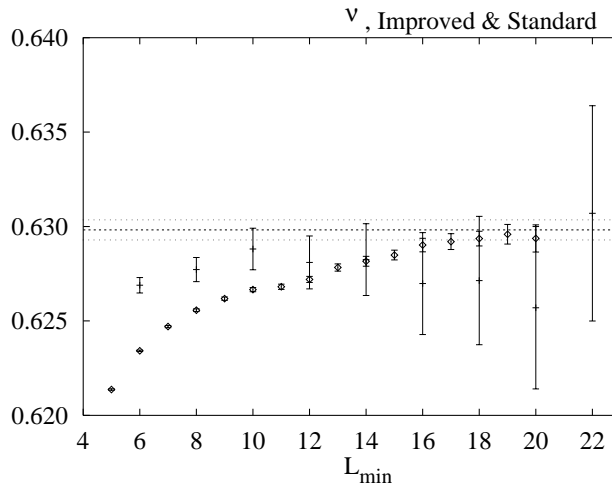


Figure 12: Fits of the energy with eq. (50) for both actions (without correction to scaling).

## 6 Comparison with Other Estimates

It is interesting to compare our estimates with other ones available from the literature. Note that extensive tables with many data from literature and experiment can be found in refs. [6], [11], and [19].

Some of the more recent estimates for the  $\nu$  and  $\eta$  exponents, together with the critical coupling of the standard Ising model are collected in table 24. Our estimates are given in the last two lines: the upper one gives to the estimates obtained with the standard action (SA) while the lower one those from the improved spin-1 action (IA). The underlined estimates are obtained by choosing our best estimate from the improved action and adding the statistical and systematic error estimates in order to obtain the overall uncertainty.

The value we obtained for the Binder cumulant from the improved action  $Q = 0.62393(13)[35]\{5\}$  can be compared with the estimate  $Q = 0.6233(4)$  of ref. [6]. It is reassuring that the high precision estimates of the recent years seem to be nicely consistent with each other.

| Ref.    | Method     | $\nu$               | $\eta$           | $\beta_c$          |
|---------|------------|---------------------|------------------|--------------------|
| [11]    | EPS        | 0.6293(26)          | 0.036(6)         |                    |
| [11]    | 3D FT      | 0.6304(13)          | 0.0335(25)       |                    |
| [20]    | 3D FT      | 0.6301(5)           | 0.0355(9)        |                    |
| [19]    | HT         | 0.6310(5)           |                  |                    |
| [21]    | MC         | 0.6308(10)          |                  |                    |
| [6, 10] | MC         | 0.6301(8)           | 0.037(3)         | 0.2216544(3)[3]    |
| [8]     | MC         | 0.6294(5)[5]        | 0.0374(6)[6]     | 0.22165456(15)[5]  |
| SA      | MC, $R'_1$ | 0.63014(54){55}     |                  | 0.22165431(19){15} |
| SA      | MC, $R'_2$ | 0.62973(43){46}{14} |                  | 0.22165405(23){25} |
| SA      | MC, $\chi$ |                     | 0.0366(8){9}     |                    |
| IA      | MC, $R'_2$ | 0.62982(22)[16]{15} |                  |                    |
| IA      | MC, $R'_2$ | <u>0.6298(5)</u>    |                  |                    |
| IA      | MC, $R'_1$ | 0.62988(51)[32]{51} |                  |                    |
| IA      | MC, $\chi$ |                     | 0.0366(6)[2]     |                    |
| IA      | MC, $\chi$ |                     | <u>0.0366(8)</u> |                    |

Table 24: Results of the present study from standard (SA) and improved (IA) actions are compared with other estimates: from  $\epsilon$ -expansion (EPS), field theory calculations in three dimensions (3D FT), high temperature expansions (HT) and Monte Carlo simulations (MC). The underlined estimates for the critical exponents are our best estimates together with error estimates which give the overall uncertainty, including systematic effects.

## 7 Conclusions

By performing a detailed comparison with high precision results of the standard action, we have demonstrated that the spin-1 Ising model with suitably tuned coupling constants has remarkably improved finite size scaling properties. We obtained estimates of very high precision for the critical exponents  $\nu$  and  $\eta$  and two other universal quantities, the Binder cumulant  $Q$  and the ratio of partition functions  $Z_a/Z_p$ .

All estimates from the two different actions are consistent with each other. In spite of the higher statistics and the bigger lattice sizes of the standard action data, the estimates from the improved action are by far more precise. In particular, c.f. table 24, the systematic errors are smaller for the improved action than for the standard action.

The authors of refs. [8, 9] claim that an improvement of the action as discussed in this paper and in ref. [9] does not allow for more precise estimates of universal quantities such as the critical exponents. In their argument they ignore the fact that ratios of correction amplitudes are universal. Once these ratios are computed for the standard Ising model, where the corrections are large, they allow for powerful bounds in the case of the improved action. E.g., leading order corrections to scaling of the Binder cumulant are much stronger than those of the derivative of the Binder cumulant. Therefore it is quite clear, that we can safely ignore  $L^{-\omega}$  corrections in the analysis of  $Q'$  obtain from the improved model.

It would be worthwhile to use the present model in studies of physical quantities not discussed in this work and to check to what extent the improved scaling behaviour helps to get better estimates.

An interesting question is whether and to what extent the improvement that we have achieved can be further enhanced. It seems tempting to study models with even more couplings in order to systematically reduce the effects from next-to-leading corrections to scaling. However, little is known about these higher order corrections, and one does not really know how many parameters would be necessary to remove corrections of order  $L^{-x}$ , with  $x \approx 2$ . Note that at that level of improvement also the question of improved observables comes into play. We thus believe that the improvement with two parameters which we performed is the optimal thing one can do in a systematic way. Note that our improvement also eliminates subleading corrections of the type  $L^{-n\omega}$ , cf. the discussion in section 5.

Last but not least, application of the ideas underlying the present analysis

to other models seems very promising.

## References

- [1] V. Privman, in: *Finite Size Scaling and Numerical Simulations of Statistical Systems*, V. Privman, ed., World Scientific, Singapore, 1990.
- [2] K.G. Wilson and J.B. Kogut, *Phys. Rep.* C 12 (1974) 75; K.G. Wilson, *Rev. Mod. Phys.* 47 (1975) 773; K.G. Wilson, *Rev. Mod. Phys.* 55 (1983) 583.
- [3] The first article on this issue is P. Hasenfratz and F. Niedermayer, *Nucl. Phys. B* 214 (1994) 785. An up to date reference list can be found in P. Hasenfratz, hep-lat/9803027.
- [4] K. Symanzik, *Nucl. Phys. B* 226 (1987) 187; K. Symanzik, *Nucl. Phys. B* 226 (1987) 205.
- [5] See, e.g., the various contributions to the LATTICE 97 Symposium, parallel session *Improvement and Renormalisation*, *Nucl. Phys. B (Proc. Suppl.)* 63 (1998), pp. 847-933.
- [6] H.W.J. Blöte, E. Luijten, and J.R. Heringa, *J. Phys. A* 28 (1995) 6289, cond-mat/9509016.
- [7] M. Hasenbusch, K. Pinn, and S. Vinti, cond-mat/9804186.
- [8] H.G. Ballesteros, L.A. Fernández, V. Martín-Mayor, A. Muñoz Sudupe, G. Parisi, and J.J. Ruiz-Lorenzo, cond-mat/9805125.
- [9] H.G. Ballesteros, L.A. Fernández, V. Martín-Mayor, A. Muñoz Sudupe, hep-lat/9805022.
- [10] A.L. Talapov and H.W.J. Blöte, *J. Phys. A* 29 (1996) 5727, cond-mat/9603013.
- [11] R. Guida and J. Zinn-Justin, cond-mat/9803240.
- [12] M. Creutz, *Phys. Rev. Lett.* 50 (1983) 1411.
- [13] K. Rummukainen, *Nucl. Phys. B* 390 (1993) 621.

- [14] M. Hasenbusch, in preparation.
- [15] U. Wolff, Phys. Lett. B 228 (1989) 379.
- [16] M. Hasenbusch, Physica A 197 (1993) 423.
- [17] A. Aharony, P.C. Hohenberg, and V. Privman, in: Phase transitions and critical phenomena, Vol. 14, C. Domb and J.L. Lebowitz, eds., Academic Press 1991.
- [18] H.G. Ballesteros, L.A. Fernández, V. Martín-Mayor, A. Muñoz Sudupe, G. Parisi, and J.J. Ruiz-Lorenzo, Phys. Lett. B 400 (1997) 346.
- [19] P. Butera and M. Comi, Phys. Rev. B 56 (1997) 8212, hep-lat/9703018. An estimate for  $\eta$  may be obtained using  $\gamma = 1.2385(5)$  and the relation  $\eta = 2 - \gamma/\nu$ .
- [20] Results by Murray and Nickel, taken from table 10 of [11]. Errors from uncertainty of  $\tilde{g}^*$  are not taken into account.
- [21] M. Hasenbusch and K. Pinn, cond-mat/9706003, to appear in J. Phys. A. In this work, also  $\alpha = 0.1115(37)$  is obtained.

## Appendix: Basic Monte Carlo Results

### Standard Action

| $L$ | $Z_a/Z_p$    | $Q$           | $\chi/L^2$   | $E_{NN}$      |
|-----|--------------|---------------|--------------|---------------|
| 4   |              | 0.6597860(58) | 1.324852(21) | 0.4310732(41) |
| 5   |              | 0.6537418(59) | 1.350645(22) | 0.4047035(33) |
| 6   | 0.550587(31) | 0.6492132(60) | 1.363074(23) | 0.3881589(27) |
| 7   |              | 0.6458092(62) | 1.369365(24) | 0.3769937(24) |
| 8   | 0.549195(34) | 0.6431935(72) | 1.372565(28) | 0.3690452(23) |
| 9   |              | 0.6411374(85) | 1.374004(34) | 0.3631459(23) |
| 10  | 0.548166(50) | 0.6394995(96) | 1.374541(37) | 0.3586312(22) |
| 11  |              | 0.6381157(99) | 1.374188(38) | 0.3550664(20) |
| 12  | 0.547379(52) | 0.636980(11)  | 1.373593(41) | 0.3522077(19) |
| 13  |              | 0.636038(15)  | 1.372799(58) | 0.3498712(24) |
| 14  | 0.546851(71) | 0.635224(17)  | 1.371762(63) | 0.3479251(23) |
| 15  |              | 0.634494(18)  | 1.370545(66) | 0.3462842(22) |
| 16  | 0.546212(76) | 0.633875(19)  | 1.369375(69) | 0.3448912(21) |
| 17  |              | 0.633329(20)  | 1.368077(72) | 0.3436884(20) |
| 18  |              | 0.632816(23)  | 1.366696(80) | 0.3426440(20) |
| 19  |              | 0.632386(24)  | 1.365440(83) | 0.3417330(19) |
| 20  | 0.54587(12)  | 0.631947(89)  | 1.36379(31)  | 0.3409214(70) |
| 24  | 0.54552(12)  | 0.630659(82)  | 1.35886(28)  | 0.3384943(49) |
| 28  | 0.54512(13)  | 0.629767(93)  | 1.35386(32)  | 0.3368733(46) |
| 32  | 0.54499(12)  | 0.62906(14)   | 1.34917(40)  | 0.3357286(49) |
| 40  | 0.54447(21)  | 0.62805(15)   | 1.34171(52)  | 0.3342390(47) |
| 48  | 0.54432(20)  | 0.62720(17)   | 1.33415(58)  | 0.3333177(42) |
| 56  | 0.54383(32)  | 0.62705(23)   | 1.32848(81)  | 0.3327115(48) |
| 64  | 0.54354(30)  | 0.62690(23)   | 1.32378(82)  | 0.3322842(41) |
| 80  | 0.54373(51)  | 0.62568(34)   | 1.3144(13)   | 0.3317204(49) |
| 96  | 0.54263(49)  | 0.62585(36)   | 1.3079(13)   | 0.3313780(38) |
| 112 | 0.54546(83)  | 0.62412(64)   | 1.2969(20)   | 0.3311406(48) |
| 128 | 0.54337(80)  | 0.62518(62)   | 1.2921(22)   | 0.3309828(45) |

Table 25: Results for  $R_1 = Z_a/Z_p$ ,  $R_2 = Q$ , the susceptibility  $\chi$  divided by  $L^2$ , and the energy per link,  $E_{NN}$ , at  $\beta = 0.2216545$ .

**Improved action**

| $L$ | $Z_a/Z_p$   | $Q$         | $\chi/L^2$  |
|-----|-------------|-------------|-------------|
| 4   | 0.53599(07) | 0.62408(05) | 0.87609(13) |
| 6   | 0.54080(07) | 0.62491(06) | 0.88104(14) |
| 8   | 0.54193(09) | 0.62460(07) | 0.87706(16) |
| 10  | 0.54209(18) | 0.62464(13) | 0.87272(33) |
| 12  | 0.54248(19) | 0.62416(14) | 0.86778(35) |
| 14  | 0.54230(21) | 0.62426(15) | 0.86399(38) |
| 16  | 0.54263(17) | 0.62409(13) | 0.86000(32) |
| 18  | 0.54251(23) | 0.62410(17) | 0.85697(42) |
| 20  | 0.54286(28) | 0.62379(21) | 0.85332(50) |
| 22  | 0.54244(30) | 0.62404(23) | 0.85115(55) |
| 24  | 0.54229(23) | 0.62402(17) | 0.84914(43) |
| 28  | 0.54245(31) | 0.62386(23) | 0.84373(55) |
| 32  | 0.54259(31) | 0.62390(23) | 0.84010(56) |
| 36  | 0.54213(41) | 0.62420(30) | 0.83742(73) |
| 40  | 0.54227(32) | 0.62403(23) | 0.83392(56) |
| 48  | 0.54250(39) | 0.62395(29) | 0.82803(69) |
| 56  | 0.54272(63) | 0.62382(47) | 0.82351(12) |

Table 26: Results for  $R_1 = Z_a/Z_p$ ,  $R_2 = Q$ , and the susceptibility  $\chi$  divided by  $L^2$ , at  $\beta = 0.383245$ .

**Improved Action**

| $L$ | $E_{NN}$     | $E_D$        | $E$          |
|-----|--------------|--------------|--------------|
| 4   | 0.283630(29) | 0.647597(17) | 1.091901(43) |
| 6   | 0.248854(18) | 0.633033(10) | 1.152537(28) |
| 8   | 0.233532(15) | 0.626493(8)  | 1.178885(24) |
| 10  | 0.225261(23) | 0.622948(12) | 1.193062(36) |
| 12  | 0.220134(19) | 0.620744(9)  | 1.201829(31) |
| 14  | 0.216748(18) | 0.619288(9)  | 1.207619(28) |
| 16  | 0.214326(12) | 0.618243(6)  | 1.211750(19) |
| 18  | 0.212558(14) | 0.617481(7)  | 1.214768(22) |
| 20  | 0.211181(15) | 0.616886(7)  | 1.217115(24) |
| 22  | 0.210132(14) | 0.616434(7)  | 1.218905(23) |
| 24  | 0.209291(10) | 0.616073(5)  | 1.220344(16) |
| 28  | 0.207992(10) | 0.615514(5)  | 1.222565(17) |
| 32  | 0.207084(9)  | 0.615120(4)  | 1.224110(14) |
| 36  | 0.206428(10) | 0.614838(5)  | 1.225227(16) |
| 40  | 0.205910(7)  | 0.614613(3)  | 1.226109(11) |
| 48  | 0.205183(6)  | 0.614299(3)  | 1.227350(11) |
| 56  | 0.204704(9)  | 0.614094(4)  | 1.228169(14) |

Table 27: Results for energy  $E_{NN}$ ,  $E_D$  and  $E$ , at  $\beta = 0.383245$ .

**Standard Action**

| $L$ | $f(L) dR_1/d\beta$ | $f(L) dR_2/d\beta$ |
|-----|--------------------|--------------------|
| 4   |                    | 0.868988(29)       |
| 5   |                    | 0.866166(30)       |
| 6   | -1.45953(13)       | 0.863364(31)       |
| 7   |                    | 0.860978(32)       |
| 8   | -1.47001(13)       | 0.859086(37)       |
| 9   |                    | 0.857510(44)       |
| 10  | -1.47311(18)       | 0.856291(50)       |
| 11  |                    | 0.855176(52)       |
| 12  | -1.47435(26)       | 0.854265(56)       |
| 13  |                    | 0.853443(79)       |
| 14  | -1.47492(26)       | 0.852892(87)       |
| 15  |                    | 0.852278(93)       |
| 16  | -1.47560(30)       | 0.851801(97)       |
| 17  |                    | 0.85112(10)        |
| 18  |                    | 0.85076(12)        |
| 19  |                    | 0.85033(12)        |
| 20  | -1.47517(44)       | 0.84968(52)        |
| 24  | -1.47462(45)       | 0.84937(51)        |
| 28  | -1.47396(51)       | 0.84789(58)        |
| 32  | -1.47305(64)       | 0.84710(72)        |
| 40  | -1.47400(84)       | 0.84641(94)        |
| 48  | -1.4737(14)        | 0.8462(10)         |
| 56  | -1.4714(13)        | 0.8457(14)         |
| 64  | -1.4756(16)        | 0.8454(15)         |
| 80  | -1.4749(20)        | 0.8479(21)         |
| 96  | -1.4721(49)        | 0.8451(24)         |
| 112 | -1.4716(37)        | 0.8451(41)         |
| 128 | -1.4727(53)        | 0.8433(41)         |

Table 28: Results for derivatives of  $R_1 = Z_a/Z_p$ ,  $R_2 = Q$ , with respect to  $\beta$ , multiplied by the factor  $f(L) = L^{-1/0.63}$ , at  $\beta = 0.2216545$ .

**Improved Action**

| $L$ | $f(L) \partial R_1 / \partial \beta$ | $f(L) dR_1 / d\beta$ | $f(L) \partial R_2 / \partial \beta$ | $f(L) dR_2 / d\beta$ |
|-----|--------------------------------------|----------------------|--------------------------------------|----------------------|
| 4   | -1.09974(17)                         | -.63210(11)          | .65894(15)                           | -.09882(03)          |
| 6   | -1.13595(17)                         | -.64829(10)          | .66236(15)                           | -.09685(03)          |
| 8   | -1.14621(20)                         | -.65290(12)          | .66295(18)                           | -.09614(03)          |
| 10  | -1.15051(41)                         | -.65498(24)          | .66276(37)                           | -.09577(07)          |
| 12  | -1.15293(45)                         | -.65567(25)          | .66307(40)                           | -.09571(07)          |
| 14  | -1.15385(49)                         | -.65661(27)          | .66310(46)                           | -.09555(08)          |
| 16  | -1.15432(44)                         | -.65652(25)          | .66290(39)                           | -.09554(07)          |
| 18  | -1.15547(59)                         | -.65692(33)          | .66294(55)                           | -.09545(11)          |
| 20  | -1.15603(71)                         | -.65732(39)          | .66322(64)                           | -.09553(11)          |
| 22  | -1.15542(79)                         | -.65714(43)          | .66310(74)                           | -.09574(17)          |
| 24  | -1.15675(61)                         | -.65790(34)          | .66419(55)                           | -.09568(11)          |
| 28  | -1.15565(80)                         | -.65730(44)          | .66199(75)                           | -.09520(20)          |
| 32  | -1.15664(82)                         | -.65793(46)          | .66283(75)                           | -.09523(18)          |
| 36  | -1.1568(12)                          | -.65776(61)          | .6638(11)                            | -.09525(49)          |
| 40  | -1.15665(84)                         | -.65785(47)          | .66326(84)                           | -.09557(37)          |
| 48  | -1.1563(11)                          | -.65752(59)          | .6635(11)                            | -.09513(58)          |
| 56  | -1.1562(17)                          | -.65739(97)          | .6628(19)                            | -.0958(12)           |

Table 29: Results for partial and total derivatives of  $R_i$ , multiplied by the factor  $f(L) = L^{-1/0.63}$ , at  $\beta = 0.383245$ .